Quantifying atmospheric nitrogen deposition through a nationwide monitoring network across China

W. Xu[1], X. S. Luo[1,2], Y. P. Pan[3], L. Zhang[4], A. H. Tang[1], J. L. Shen[5], Y. Zhang[6], K. H. Li[7], Q. H. Wu[1], D. W. Yang[1], Y. Y. Zhang[1], J. Xue[1], W. Q. Li[8], Q. Q. Li[1,9], L. Tang[9], S. H. Lu[10], T. Liang[11], Y. A. Tong[11], P. Liu[12], Q. Zhang[12], Z. Q. Xiong[13], X. J. Shi[14], L. H. Wu[15], W. Q. Shi[16], K. Tian[17], X. H. Zhong[17], K. Shi[18], Q. Y. Tang[19], L. J. Zhang[20], J. L. Huang[21], C. E. He[22], F. H. Kuang[23], B. Zhu[23], H. Liu[24], X. Jin[25], Y. J. Xin[25], X. K Shi[26], E. Z. Du[27], A. J. Dore[28], S. Tang[28], J. L. Jr. Collett[29], K. Goulding[30], Y. X. Sun[31], J. Ren[32], F. S. Zhang[1], X. J. Liu[1,*]

[1]College of Resources and Environmental Sciences, China Agricultural University, Beijing 100193, China

[2]Institute of Plant Nutrition, Resources and Environmental Sciences, Henan Academy of Agricultural Sciences, Zhengzhou 450002, China

[3]State Key Laboratory of Atmospheric Boundary Layer Physics and Atmospheric Chemistry (LAPC), Institute of Atmospheric Physics, Chinese Academy of Sciences, Beijing 100029, China

[4]Laboratory for Climate and Ocean-Atmosphere Studies, Department of Atmospheric and Oceanic Sciences, School of Physics, Peking University, Beijing 100871, China

[5]Institute of Subtropical Agriculture, Chinese Academy of Sciences, Changsha 4410125, China

[6]College of Nature Conservation, Beijing Forestry University, Beijing 100083, China

[7]Xinjiang Institute of Ecology and Geography, Chinese Academy of Sciences, Urumqi 830011, China

[8]Fujian Institute of Tobacco Agricultural Sciences, Fuzhou 350003, China

[9]College of Resources and Environmental Sciences, Yunnan Agricultural University, Kunming 650224, China

[10]Soil and Fertilizer Institute, Sichuan Academy of Agricultural Sciences, Chengdu 610066, China

[11]Nature Resource and Environment College, Northwest A&F University, Yangling 712100, China

[12]Institute of Agricultural Environment and Resource, Shanxi Academy of Agricultural Sciences, Taiyuan 030031, China

[13]College of Resources and Environmental Sciences, Nanjing Agricultural University, Nanjing 210009, China

[14]College of Resources and Environment, Southwest University, Chongqing 400716, China

[15]College of Environmental and Resource Sciences, Zhejiang University, Hangzhou 310029, China

[16]South Subtropical Crops Research Institute, Chinese Academy of Tropical Agricultural Science, Zhanjiang 524091, China

[17]Rice Research Institute, Guangdong Academy of Agricultural Sciences, Guangzhou 510640, China

[18]College of Environmental and Chemical Engineering, Dalian Jiaotong University, Dalian

116028, China
[19]College of Agriculture, Hunan Agricultural University, Changsha 410128, China
[20]College of Resources and Environment, Agricultural University of Hebei, Baoding 071001, China
[21]College of Plant Science and Technology, Huazhong Agricultural University, Wuhan, China
[22]Institute of Geographic Sciences and Natural Resources, Chinese Academy of Sciences, Beijing 100101, China
[23]Institute of Mountain, Hazards and Environment, Chinese Academy of Sciences, Chengdu 610041, China
[24]Research Institute of Soil & Fertilizer and Agricultural Water Conservation, Xinjiang Academy of Agricultural Sciences, Urumqi 830091, China
[25]The Bureau of Qinghai Meteorology, Xining 810001, China
[26]Agriculture, Forestry and Water Department of Changdao County, Changdao 265800, China
[27]State Key Laboratory of Earth Surface Processes and Resource Ecology, and College of Resources Science & Technology, Beijing Normal University, Beijing 100875, China
[28]Centre for Ecology & Hydrology Edinburgh, Bush Estate, Penicuik, Midlothian EH26 0QB, UK
[29]Department of Atmospheric Science, Colorado State University, Fort Collins, CO 80523, USA
[30]The Sustainable Soils and Grassland Systems Department, Rothamsted Research, Harpenden AL5 2JQ, UK
[31]Institute of Soil and Fertilizer, Anhui Academy of Agricultural Sciences, Hefei 230031, China
[32]Institute of Soil and Fertilizer, Jilin Academy of Agricultural Sciences, Changchun 130124, China
Corresponding author: liu310@cau.edu.cn (X. J. Liu).

Abstract: A Nationwide Nitrogen Deposition Monitoring Network (NNDMN) containing forty-three monitoring sites was established in China to measure gaseous NH_3, NO_2 and HNO_3 and particulate NH_4^+ and NO_3^- in air and/or precipitation from 2010 to 2014. Wet/bulk deposition fluxes of N_r species were collected by precipitation gauge method and measured by continuous flow analyzer; dry deposition fluxes were estimated using airborne concentration measurements and inferential models. Our observations reveal large spatial variations of atmospheric N_r concentrations and dry and wet/bulk N_r deposition. On a national basis, the annual average concentrations (1.3-47.0 μg N m^{-3}) and dry plus wet/bulk deposition fluxes (2.9-83.3 kg N ha^{-1} yr^{-1}) of inorganic N_r species ranked by land use as urban > rural > background sites and by regions as north China > southeast China > southwest China > northeast China > northwest China > Tibetan Plateau, reflecting the impact of

anthropogenic N_r emission. Average dry and wet/bulk N deposition fluxes were 20.6 ± 11.2 (mean ± standard deviation) and 19.3 ± 9.2 kg N ha^{-1} yr^{-1} across China, with reduced N deposition dominating both dry and wet/bulk deposition. Our results suggest atmospheric dry N deposition is equally important to wet/bulk N deposition at the national scale. Therefore both deposition forms should be included when considering the impacts of N deposition on environment and ecosystem health.

Keywords: air pollution; reactive nitrogen; dry deposition; wet deposition; ecosystem; China

1. Introduction

Humans continue to accelerate the global nitrogen (N) cycle at a record pace as rates of anthropogenic reactive nitrogen (N_r) fixation have increased 20-fold over the last century (Galloway et al., 2008). New N_r from anthropogenic fixation is formed primarily through cultivation of N-fixing legumes, the Haber-Bosch process and combustion of fossil-fuel (Galloway et al., 2013). As more N_r have been created, emissions of N_r (NO_x=NO+NO_2, and NH_3) to the atmosphere have increased from approximately 34 Tg N yr^{-1} in 1860 to 109 Tg N yr^{-1} in 2010 (Fowler et al., 2013; Galloway et al., 2004); most of this emitted N_r is deposited back to land and water bodies. As an essential nutrient, N supplied by atmospheric deposition is useful for all life forms in the biosphere and may stimulate primary production in an ecosystem if it does not exceed the ecosystem-dependent critical load (Liu et al., 2010, 2011). However, long-term high levels of atmospheric N_r and its deposition can reduce biological diversity (Clark et al., 2008), degrade human health (Richter et al., 2005), alter soil and water chemistry (Vitousek et al., 1997) and influence the greenhouse gas balance (Matson et al., 2002).

Nitrogen deposition occurs via dry and wet processes. Neglecting dry deposition can lead to substantial underestimation of total flux as dry deposition can contribute up to 2/3 of total N deposition (Flechard et al., 2011; Vet et al., 2014). For quantification of atmospheric deposition at the national scale, long-term monitoring networks such as CAPMoN (Canada), IDAF (Africa), CASTNET/NADP (the United States), EMEP (Europe) and EANET (East Asia) have been established; such networks are essential for quantification of both wet and dry deposition and revealing long-term trends and spatial patterns under major environmental and climate change (Skeffington and Hill, 2012). Wet deposition, by means of rain or snow, is relatively easily measured in existing networks. In contrast, dry deposition of gases and particulate matter is much

more difficult to measure, and strongly influenced by factors such as surface roughness, surface wetness, and climate and environmental factors (Erisman et al., 2005). Direct methods (e.g., eddy correlation, chambers) and indirect methods (e.g., inferential, gradient analysis) can determine dry deposition fluxes (Seinfeld and Pandis, 2006). The inferential method is widely used in many monitoring networks (e.g. CASTNET and EANET), where dry deposition rates are derived from measured ambient concentrations of N_r species and computed deposition velocities (Endo et al., 2011; Holland et al., 2005; Pan et al., 2012). Additionally, atmospheric modeling has been used as an operational tool to upscale results from sites to regions where no measurements are available (Flechard et al., 2011; Zhao et al., 2015).

According to long-term trends observed by the above monitoring networks, N deposition has decreased over the last two decades in Europe (EEA, 2011). Measurements of wet deposition in the US show a strong decrease in NO_3-N deposition over most of the country (Du et al., 2014), but NH_4-N deposition increased in agricultural regions. China, as one of the most rapidly developing countries in East Asia, has witnessed serious atmospheric N_r pollution since the late 1970s (Hu et al., 2010; Liu et al., 2011). Accurate quantification of N deposition is key to assessing its ecological impacts on terrestrial ecosystems (Liu et al., 2011). Previous modeling studies (e.g., Dentener et al., 2006; Galloway et al., 2008; Vet et al., 2014) suggested that central-east China was a global hotspot for N deposition. More recently, based on meta-analyses of historic literature, both Liu et al. (2013) and Jia et al. (2014) reported a significant increase in N wet/bulk deposition in China since the 1980s or 1990s. However, most measurements in China only reported wet/bulk deposition (e.g., Chen et al., 2007; Huang et al., 2013; Zhu et al., 2015) and/or dry deposition (Luo et al., 2013; Shen et al., 2009; Pan et al., 2012) at a local or regional scale. Although national N deposition has been investigated by Lü and Tian (2007, 2014), the deposition fluxes were largely underestimated due to the inclusion only of gaseous NO_2 in dry deposition and not NH_3, HNO_3 and particulate ammonium and nitrate etc. Therefore, the magnitude and spatial patterns of *in-situ* measured N wet /bulk and dry deposition across China are still not clear.

Against such a background, we have established a Nationwide Nitrogen Deposition Monitoring Network (NNDMN) in China since 2010, measuring both wet/bulk and dry deposition. The NNDMN consists of forty-three *in-situ* monitoring sites, covering urban, rural (cropland) and background (coastal, forest and grassland) areas across

China. The focus of the network is to conduct high-quality measurements of atmospheric N_r in gases, particles and precipitation. These data provide a unique and valuable quantitative description of N_r deposition in China, but have never been published as a whole. The objectives of this study were therefore to: (1) obtain the first quantitative information on atmospheric N_r concentrations and pollution status across China; and (2) analyze overall fluxes and spatial variations of N wet/bulk and dry deposition in relation to anthropogenic N_r emissions from different regions.

2. Materials and Methods

2.1 Sampling sites

The distribution of the forty-three monitoring sites in the NNDMN is shown in **Fig. 1**. Although sampling periods varied between sites, most of our monitoring started from 2010 to 2014 (see Supporting Materials for details). The NNDMN comprise 10 urban sites, 22 rural sites and 11 background sites (**Table S1** of the online Supplement). To better analyze atmospheric N deposition results among the sites, we divided the forty-three sites into six regions: north China (NC, 13 sites), northeast China (NE, 5 sites); northwest China (NW, 6 sites), southeast China (SE, 11 sites), southwest China (SW, 6 sites), and Tibetan Plateau (TP, 2 sites), representing China's various social-economical and geo-climatic regions (for details, see **Sect. A1** of the online Supplement). The sites in the six regions are described using region codes (i.e., NC, NE, NW, SE, SW, TP) plus site numbers such as NC1, NC2, NC3, ..., NE1, NE2, etc. The longitudes and latitudes of all 43-sites ranged from 83.71 to 129.25 ºE, and from 21.26 to 50.78 ºN, respectively. Annual mean rainfall ranged from 170 to 1748 mm and the annual mean air temperature ranged from -6.2 to 23.2 °C. Site names, land use types and population densities are summarized in **Table S1** of the Supplement. More detailed information on the monitoring sites, such as specific locations, surrounding environment and possible emission sources are provided in **Sect. A2** of the Supplement.

2.2 Collection of gaseous and particulate N_r samples

In this study ambient N_r concentrations of gaseous NH_3, NO_2 and HNO_3, and particulate NH_4^+ (pNH_4^+) and NO_3^- (pNO_3^-) were measured monthly at the 43 sites using continuous active and passive samplers. DELTA active sampling systems (DEnuder for Long-Term Atmospheric sampling, described in detail in Flechard et al. (2011) and Sutton et al. (2001)), were used to collect NH_3, HNO_3, pNH_4^+ and pNO_3^-; NO_2 samples were collected using Gradko diffusion tubes (Gradko International

Limited, UK) at all sampling sites. The air intakes of the DELTA system and the NO_2 tubes were set at a height of 2 m above the ground (at least 0.5 m higher than the canopy height) at most sites. At a few sites, the DELTA systems could not be used due to power constraints. Therefore, NH_3 samples were collected using ALPHA passive samplers (Adapted Low-cost High Absorption, designed by the Center for Ecology and Hydrology, Edinburgh, UK), while the pNH_4^+ and pNO_3^- in PM_{10} were collected using particulate samplers (TSH-16 or TH-150III, Wuhan Tianhong Corp., Wuhan, China). However, HNO_3 measurements were not performed due to lack of corresponding passive samplers. Briefly, all the measurements of N_r concentration were based on monthly sampling (one sample per month for each N_r species) except at the very few sites without DELTA systems, where pNH_4^+ and pNO_3^- samples were calculated from daily sampling transformed to monthly averaged data. Detailed information on measuring methods, sample replication and collection are given in **Sect. A3** of the Supplement with sampling periods listed in **Table S2** of the Supplement. Comparisons between the ALPHA samplers and the DELTA systems at six network sites for gaseous NH_3 measurements indicated that the two methods provided comparable NH_3 concentrations (values between the two methods were not significantly different) (cf. **Sect. A4** in the Supplement and **Fig. S1** therein).

2.3 Collection of precipitation

At all monitoring sites precipitation (here we define it as wet/bulk deposition which contains wet and part dry deposition) samples were collected using precipitation gauges (SDM6, Tianjin Weather Equipment Inc., China) located beside the DELTA systems (c. 2 m). The collector, consisting of a stainless steel funnel and glass bottle (vol. 2000-2500 ml), collects precipitation (rainwater, snow) without a power supply. Precipitation amount was measured using a graduated cylinder (scale range: 0-10 mm; division: 0.1 mm) coupled with the gauge. After each daily (8:00 am-8:00 am next day) event, the collected samples were thoroughly mixed and then immediately stored in clean polyethylene bottles (50 mL). All collected samples (including melted snow) samples were frozen at −18 °C at each site until delivery to the laboratory at China Agricultural University (CAU) for analysis of inorganic N (NH_4^+ and NO_3^-). The gauges were cleaned with high-purity water after each collection and once every week in order to avoid cross contamination.

2.4 Analytical procedures

In CAU's analytical laboratory, the exposed sampling trains of the DELTA systems

and passive samples were stored at 4 °C and analyzed at one-month intervals. The HNO_3 denuders and alkaline-coated filters were extracted with 10 mL 0.05 % H_2O_2 in aqueous solution. The NH_3 denuders and acid-coated filters, and ALPHA samplers were extracted with 10 mL high-purity water. The loaded PM_{10} filters were extracted with 50 mL high-purity water by ultrasonication for 30-60 min and then filtered through a syringe filter (0.45 μm, Tengda Inc., Tianjin, China). Ammonium (NH_4^+) and nitrate (NO_3^-) in the extracted and filtered solutions were measured with an AA3 continuous-flow analyzer (Bran+Luebbe GmbH, Norderstedt, Germany). The detection limits were 0.01 mg N L^{-1} for NH_4^+ and NO_3^-. It should be noted that NO_3^- was converted to NO_2^- during the chemical analysis. So, NO_2^- here was included in the analysis, and NO_3^- equals to the sum of NO_2^- and NO_3^-. The disks from the Gradko samplers were extracted with a solution containing sulphanilamide, H_3PO_4 and N-1-Naphthylethylene-diamine, and the NO_2^- content in the extract determined using a colorimetric method by absorption at a wavelength of 542 nm. The detection limit for NO_2^- was 0.01 mg N L^{-1}. Three laboratory and three field blank samples were extracted and analyzed using the same methods as the exposed samples. After correcting for the corresponding blanks, the results were used for the calculation of ambient concentrations of gaseous and particulate N_r. Each collected precipitation sample was filtered with a 0.45 μm syringe filter, and 15 mL filtrates frozen and stored in polypropylene bottles until chemical analysis within one month. The NH_4^+ and NO_3^- concentrations of the filtrates were determined using an AA3 continuous-flow analyzer as described above.

2.5 Deposition flux estimation

The inferential technique, which combines the measured concentration and a modeled dry deposition velocity (V_d), was used to estimate the dry deposition fluxes of N_r species (Schwede et al., 2011; Pan et al., 2012). The concentrations of gases (HNO_3, NO_2 and NH_3) and aerosols (NH_4^+ and NO_3^-) were measured as described in Section 2.2. The monthly average V_d over China was calculated by the GEOS-Chem chemical transport model (CTM) (Bey et al., 2001; http://geos-chem.org). The GEOS-Chem CTM is driven by GEOS-5 (Goddard Earth Observing System) assimilated meteorological data from the NASA Global Modeling and Assimilation Office (GMAO) with a horizontal resolution of 1/2° latitude × 2/3° longitude and 6-h temporal resolution (3-h for surface variables and mixing depths). We used a nested-grid version of GEOS-Chem for Asia that has the native 1/2°×2/3° resolution

over East Asia (70°E-150°E, 11°S-55°N) (Chen et al., 2009). The nested model has been applied to examine atmospheric N deposition to the northwestern Pacific (Zhao et al., 2015), and a similar nested model for North America has been used to analyze N deposition over the United States (Zhang et al., 2012a; Ellis et al., 2013). The model calculation of dry deposition of N_r species follows a standard big-leaf resistance-in-series model as described by Wesely (1989) for gases and Zhang et al. (2001) for aerosol. For a detailed description of the V_d calculation as well as the estimation of N dry deposition, the reader is referred to the Supplement (**Sect. A5**), with monthly and annual dry deposition velocities of N_r for different land use types presented in **Tables S3 and S4** therein. The model uses the land map of the Global Land Cover Characteristics Data Base Version 2.0 (http://edc2.usgs.gov/glcc/globdoc2_0.php), which defines the land types (e.g., urban, forest, etc.) at the native 1 km × 1 km resolution and is then binned to the model resolution as a fraction of the grid cell covered by each land type. The model 1/2° resolution may coarsely represent the local land characteristics at the monitoring sites. Future work using a single-point dry deposition model as for CASTNET (Clarke et al., 1997) would further improve the dry deposition flux estimates, but that requires concurrent *in-situ* measurements of meteorological variables which are not available at present.

Wet/bulk N deposition flux was calculated as the product of the precipitation amount and the concentration of N_r species in precipitation, using the following equations (1) and (2):

$$C_w = \sum_{i=1}^{n}(C_i P_i)/\sum_{i=1}^{n} P_i \quad (1)$$

where C_w is the volume-weighted mean (VWM) concentration (mg N L^{-1}) calculated from the n precipitation samples within a month or a year, and the individual sample concentration C_i is weighted by the rainfall amount P_i for each sample.

$$D_w = P_t C_w /100 \quad (2)$$

where D_w is the wet/bulk deposition flux (kg N ha^{-1}), P_t is the total amount of all precipitation events (mm), and 100 is a unit conversion factor.

2.6 Statistics

A one-way analysis of variance (ANOVA) and nonparametric t-tests were conducted to examine the differences in the investigated variables between sites (urban, rural and background) and between the six regions. Linear regression analysis was used to

analyze the relationships among annual wet N deposition flux, annual precipitation amount and annual VWM concentration of inorganic N in precipitation. All analyses were performed using SPSS 11.5 (SPSS Inc., Chicago, IL, USA). Statistically significant differences were set at P values < 0.05.

3. Results

3.1 Concentrations of N_r species in air

Monthly mean concentrations of NH_3, NO_2, HNO_3, pNH_4^+ and pNO_3^- were 0.08-34.8, 0.13-33.4, 0.02-4.90, 0.02-55.0 and 0.02-32.1 μg N m^{-3}, respectively (**Fig. S2a-e**, Supplement). The annual mean concentrations of gaseous and particulate N_r were calculated for each site from the monthly N_r concentrations (**Fig. 2a**), and further were averaged for land use types in the six regions (**Fig. 3a-e**) and the whole nation (**Fig. 4a**) according to geographical location and the classification of each site.

Annual mean NH_3 concentrations ranged from 0.3 to 13.1 μg N m^{-3}, with an overall average value of 6.1 μg N m^{-3}. In NC, SE and SW, the NH_3 concentrations at the urban sites (average for the three regions, 9.5 ± 2.1 μg N m^{-3}) were about 1/3 higher than at the rural sites (6.2 ± 2.3 μg N m^{-3}) and were almost twice of those at the background sites (4.8 ± 1.4 μg N m^{-3}), whereas in NE and NW NH_3 concentrations were lower at the urban sites (average of the two regions, 5.5 ± 3.2 μg N m^{-3}) than at the rural sites (8.8 ± 0.3 μg N m^{-3}) but 4.6-times greater than at the background sites (1.2 ± 0.5 μg N m^{-3}). Comparing land use types by region, annual NH_3 concentrations at the rural sites in northern regions (NC, NE and NW) were approximately equal, which on average were 1.8-times greater than the average of southern rural sites. In contrast, annual NH_3 concentrations at urban and background sites ranked in the order: SW > NC > NW > SE > TP > NE, and SW > NC > SE > NW > TP > NE, respectively (**Fig. 3a**).

Annual mean NO_2 concentrations showed similar spatial variations (0.4 to 16.2 μg N m^{-3}) to those of NH_3, and overall averaged 6.8 μg N m^{-3}. In the six regions, the NO_2 concentrations at urban sites were 1.4-4.5 times higher than those at rural sites, and were even 2.0-16.6 times higher than the background sites (except for SW). By comparison among regions, annual mean NO_2 concentrations at rural sites in NC were about 2.6-times higher than in NE and NW, and overall averaged NO_2 concentrations in northern rural China (NC, NE and NW, 5.7 ± 3.5 μg N m^{-3}) were comparable to those at southern rural sites (average of SE and SW, 5.1± 0.1 μg N m^{-3}). As for urban and background sites, the annual mean NO_2 concentrations followed the order: NC >

NW > SE > SW > NE > TP, and SW > NC > SE > NE > NW > TP, respectively (**Fig. 3b**).

Annual mean HNO_3 concentrations were relatively low everywhere (from 0.1 to 2.9 μg N m^{-3}, average 1.3 μg N m^{-3}). In all regions except NE and TP, the HNO_3 concentrations were highest at the urban sites (1.7-2.4 μg N m^{-3}), followed by the rural sites (0.8-1.6 μg N m^{-3}), and were lowest at the background sites (0.2-1.1 μg N m^{-3}). The HNO_3 concentrations were comparable for the same land use types across northern and southern monitoring sites, on average, 1.8 vs. 1.8, 1.2 vs. 1.0, and 0.6 vs. 0.8 μg N m^{-3} at the urban, rural and background sites, respectively (**Fig. 3c**). The annual mean concentrations of pNH_4^+ and pNO_3^- were in the ranges of 0.2-18.0 μg N m^{-3} (average 5.7 μg N m^{-3}) and 0.2-7.7 μg N m^{-3} (average 2.7 μg N m^{-3}), respectively. Annual pNH_4^+ concentrations show a decreasing trend of urban > rural > background in all regions (except NE), where relatively higher concentrations were observed at the rural sites than the urban sites, and in SE, where no clear differences were observed among three land use types (**Fig. 3d**). In contrast, annual pNO_3^- concentrations showed a declining trend of urban > rural > background in all regions (**Fig. 3e**). Overall, annual mean concentrations of both pNH_4^+ and pNO_3^- at all land use types were both slightly higher in northern China (NC, NE and NW) than in southern China (SE, SW and TP).

In total, annual mean concentrations of gaseous and particulate N_r in air were 1.3-47.0 μg N m^{-3} among all sampling sites. The total annual concentrations of measured N_r generally decreased in the order of urban > rural > background in all regions except NE (**Fig. 3f**).

3.2 Concentrations of N_r species in precipitation

The monthly VWM concentrations of inorganic N_r species at the forty-three sampling sites during the study period ranged from 0.01 to 27.1 mg N L^{-1} for NH_4^+-N and from 0.02 to 27.9 mg N L^{-1} for NO_3^--N (**Fig. S3**, Supplement). The annual VWM concentrations of NH_4^+-N and NO_3^--N across all sites were in the ranges of 0.2-4.3 and 0.1-2.5 mg N L^{-1}, respectively, with averages of 1.6 and 1.3 mg N L^{-1} (**Fig. 2b**). The urban-rural-background distributions of annual VWM concentrations of NH_4^+-N and NO_3^--N were, respectively, fairly coincided with corresponding reduced (i.e. NH_3 and pNH_4^+) and oxidized N_r (i.e. HNO_3 and pNO_3^-) in all regions except NH_4^+-N in SE and NO_3^--N in NW (**Figs. 3g and h**). Conversely, the regional variations in annual VWM concentrations of NH_4^+-N and NO_3^--N for the three land use types were not

consistent with corresponding reduced and oxidized N_r, respectively. On a national basis, the VWM concentrations of NH_4^+-N and NO_3^--N were both decreased in the order urban ≥ rural > background (**Fig. 4b**). The annual total inorganic N (TIN) concentrations in precipitation across all sites were 0.4-6.0 mg N L^{-1}, decreasing from urban to background sites in all regions (except NE) as well as on a national basis (**Figs. 3i and 4b**)..

3.3 Dry deposition of N_r species

The dry deposition fluxes of NH_3, NO_2, HNO_3, pNH_4^+ and pNO_3^- were in the ranges of 0.5-16.0, 0.2-9.8, 0.2-16.6, 0.1-11.7 and 0.1-4.5 kg N ha^{-1} yr^{-1}, and averaged 8.2, 3.2, 5.4, 3.2 and 1.5 kg N ha^{-1} yr^{-1}, respectively (**Fig. 5a**). The total dry N deposition across all sites ranged from 1.1 to 52.2 kg N ha^{-1} yr^{-1} (average 20.6 ± 11.2 kg N ha^{-1} yr^{-1}). Gaseous N species were the primary contributors to total dry-deposited N, ranging from 60% to 96%, despite of the missing HNO_3 data at a few sites. In general, NH_3 was predominant N_r species in total dry N deposition and accounted for 24-72%, compared with 1-43% from NO_2 and 9-37% from HNO_3. Comparing land use types in each region, spatial pattern of individual fluxes is fairly consistent with that of their respective concentrations except that of NH_3 for NC, that of NO_2 for SW, those of NO_2 and pNH_4^+ for NW and those of almost all measured N_r species for NE (**Figs. 3a-e and 6a-e**). Furthermore, a consistent picture is also seen for the total flux (sum of fluxes of five N_r species) at each land use type (**Figs. 5f and 6f**). Among the six regions, regional variations of individual fluxes at each land use type generally differed from those of their respective concentrations. Similarly, the inconsistent behavior appeared for the total fluxes at urban and rural sites but not at background site. On a national basis, there was no significant difference (p>0.05) in the total dry N deposition fluxes between urban (26.9 kg N ha^{-1} yr^{-1}) and rural (23.0 kg N ha^{-1} yr^{-1}) sites, both of which were significantly higher than background site (10.1 kg N ha^{-1} yr^{-1}). Also, a similar pattern was found for the dry deposition flux of each N_r species among different land use types (**Fig. 4c**).

3.4 Wet/bulk deposition of N_r species

Wet/bulk N deposition fluxes at the forty-three sites ranged from 1.0 to 19.1 kg N ha^{-1} yr^{-1} for NH_4^+-N and from 0.5 to 20.1 kg N ha^{-1} yr^{-1} for NO_3^--N (**Fig. 5b**). The annual wet/bulk deposition fluxes of NH_4^+-N were, on average, 1.3 times those of NO_3^--N. The total wet/bulk N (NH_4^+-N+ NO_3^--N) deposition fluxes across all the sites were

1.5-32.5 kg N ha^{-1} yr^{-1} (average 19.3 kg N ha^{-1} yr^{-1}), with a large spatial variation. Region variation of annual wet/bulk N deposition followed the order of NC > SE > SW > NE > NW > TP for NH_4^+-N, and SE > NC > SW > NE > TP > NW for NO_3^--N, both of which differed from their orders of annual VWM concentration, reflecting differences in annual precipitation amount. Annual total wet/bulk N deposition fluxes averaged 24.6, 13.6, 7.4, 24.4, 17.6 and 7.6 kg N ha^{-1} yr^{-1}, respectively, in NC, NE, NW, SE, SW and TP (**Fig. 5b**). At national scale, annual wet/bulk deposition fluxes of total inorganic N and/or each N_r species at urban and rural sites were comparable but significantly higher (p<0.05) than those at background sites **(Fig. 4d**).

3.5 Total annual dry and wet/bulk deposition of N_r species

The total (dry plus wet/bulk) N deposition at the forty-three sites ranged from 2.9 to 83.3 kg N ha^{-1} yr^{-1} (average 39.9 kg N ha^{-1} yr^{-1}) for the period, with 23-83% dry-deposited (**Fig. 5c**). Separated by land use types or regions, total annual mean N deposition fluxes were 49.7, 44.3 and 26.0 kg N ha^{-1} at the urban, rural and background sites, or 56.2, 41.7, 37.8, 27.6, 18.8, 15.2 kg N ha^{-1} in NC, SE, SW, NE, NW and TP, respectively, reflecting different anthropogenic impacts. In our network, the NH_x (i.e. wet/bulk NH_4^+-N deposition plus dry deposition of NH_3 and particulate NH_4^+)/NO_y (wet/bulk NO_3^--N deposition plus dry deposition of NO_2, HNO_3 and particulate NO_3^-) ratio at urban sites (from 0.8 to 1.8, averaging 1.2) was not significantly different (p>0.05) from rural (from 0.5 to 2.7, averaging 1.3) and background (from 1.0 to 2.5, averaging 1.6) sites. On a regional basis, the relative importance of dry vs. wet/bulk N deposition to the total deposition were different in the six regions, 57% vs. 43% in NC, 54% vs. 46% in NE, 61% vs. 39% in NW, 42% vs. 58% in SE, 55% vs. 45% in SW, and 50% vs. 50% in TP (**Fig. 7**).

4. Discussion

4.1 Concentration of N_r species in air and precipitation

China is facing serious atmospheric N_r pollution induced by anthropogenic N_r emissions (Liu et al., 2011, 2013). The present study shows that monthly N_r concentrations of species, through comparisons among regions, have a distinct spatial variability with values significantly higher (all p<0.05) in NC and significantly lower (all p<0.05) in TP. Annual mean NH_3 and NO_2 concentrations at most sampling sites are in good agreement with the emission inventory and satellite observations by Gu et al. (2012), who reported NH_3 hotspots in the North China Plain and South Central China such as Jiangsu and Guangdong provinces, while NO_x hotspots were mainly in

more developed regions such as the Jing-Jin-Ji (Beijing-Tianjin-Hebei), the Yangtze River Delta and the Pearl River Delta. Our results confirm that NC, which consumes large quantities of fertilizers (for food production) and fossil fuel (for energy supply) (Zhang et al., 2010) experiences the most serious N_r pollution in China; TP is the least polluted region due to much less human activity. When considering different land use types, the average total annual N_r concentrations ranked urban > rural > background, with significant differences (all $p<0.05$) among them, despite site-to-site variability within regions. This reflects the dominant role of human activity on atmospheric N_r.

For individual N_r species, higher mean concentrations were observed at urban sites than at rural and background sites (**Fig. 4a**). Higher NH_3 concentration in urban areas may be associated with NH_3 emissions from biological sources, such as human, sewage disposal systems and refuse containers (Reche et al., 2002). In addition, NH_3 can be produced by over-reduction of NO in automobile catalytic converters (Behera et al., 2013), increasing ambient NH_3 concentrations in urban areas with high traffic densities. Between 2006 and 2013, the number of civil vehicles increased from 2.39 to 5.17 million in Beijing and from 0.46 to 1.72 million in Zhengzhou (CSY, 2007-2014), which is likely to have resulted in elevated NH_3 emissions. Higher NO_2 concentrations are expected in urban areas due to NO_x emissions from the combustion of fossil fuels (Li and Lin, 2000), and also lead to higher HNO_3 concentrations in urban areas via NO_2 oxidation.

The higher pNH_4^+ and pNO_3^- concentrations observed at urban sites mainly resulted from the high concentrations at the northern urban sites (NC1~3, NW1 and NW2) (**Fig. 2a and Fig. S2d, e** in Supplement). This is probably due to the fact that cities in northern China, such as Beijing and Zhengzhou in NC and Urumqi in NW, are being surrounded by intensive agricultural production. Rapid developments along with urbanization in suburban areas shorten the transport distance between NH_3 emitted from agriculture and SO_2 and NO_x emitted from fossil fuel combustion (Gu et al., 2014). This allows the pollutants to react more readily and form aerosols (e.g. $PM_{2.5}$), leading to high concentrations of pNH_4^+ and pNO_3^- near or within cities. This explanation is supported by the recent MEPC (2013) report that the annual average $PM_{2.5}$ concentrations in the cities of Beijing, Zhengzhou and Urumqi were more than twice the Chinese annual mean $PM_{2.5}$ standard value of 35 μg m^{-3}, whereas cities such as Guangzhou and Xining with little surrounding agricultural production had lower $PM_{2.5}$ concentrations. In China's 12^{th} Five Year Plan (2011–2015), nationwide

controls on NO_x emissions will be implemented along with controls on SO_2 and primary particle emissions (Wang et al., 2014). In order to better improve the regional air quality for metropolitan areas, our results suggest that strict control measures on both NH_3 and NO_x would be beneficial in NC, at least in the suburban areas.

Rural sites in this study also had relatively high concentrations of all measured N_r species in air, altogether ranking in the order of NC > NE > NW > SE > SW (**Fig. 3f**).. The higher concentrations in northern China are mainly due to the combined effect of high NH_3 emissions from N fertilized farmland (Zhang et al., 2008a) and urban air pollution (e.g. NO_2, HNO_3, pNH_4^+ and pNO_3^-) transported from population centers to the surrounding rural areas (Luo et al., 2013). The lower air concentrations of N_r species at background sites can be ascribed to the lack of both substantial agricultural and industrial emissions. Additionally, higher wind speeds occurred at some background areas (e.g. NC12, NC13 and NW4) (**Table S1**, Supplement), favoring the dispersion of atmospheric pollutants.

We found that regional variations in N_r concentrations in precipitation were not fully in accordance with ambient N_r concentrations (see Sect. 3.2) when assessed by land use types. It is commonly accepted that N concentrations in precipitation are affected by the amount of precipitation (Yu et al., 2011). Negative correlations between precipitation amount and monthly volume-weighted concentrations of NH_4^+-N and NO_3^--N were obtained by fitting exponential models in all six regions (**Fig. S4**, Supplement), indicating a dilution effect of rainwater on inorganic N concentration. The relationships were not significant (p>0.05) in NW and TP, which is probably caused by low precipitation amounts at or near the sampling sites (**Fig. S5**, Supplement). Nevertheless, dilution could explain some of the regional differences in precipitation N concentrations.

4.2 Dry and wet/bulk deposition of N_r species

A significant (p<0.001) positive correlation was observed between annual dry N deposition and total annual concentrations of atmospheric N_r species across all sites (**Fig. S6**, Supplement). Therefore, higher concentrations of N_r species at urban sites led to higher dry deposition rates compared with rural and background sites, mainly attributable to elevated N_r emissions from urban sources (e.g., non-agricultural NH_3 emissions from landfills, wastewater treatments and NO_x emissions from traffic vehicles and power plants) and rapid development of intensive agricultural production in suburban areas surrounding cities, regardless of differences in dry deposition

velocities of various N_r species in different land use types. At the national scale, dry N deposition rates contributed almost half 23-83%, averaging 52%) of the total inorganic N deposition, indicating the importance of dry deposition monitoring for comprehensive N deposition quantification.

In this study, regional variations of annual wet/bulk N deposition fluxes of NH_4^+-N, NO_3^--N and their sum showed different spatial patterns to those of corresponding annual VWM concentrations of them in precipitation (see Sect. 3.4). These findings, together with no significant differences (p>0.05) in total annual wet/bulk N deposition between NC and SE, reflect, not surprisingly, that regional wet/bulk N deposition is dependent not only on N_r concentrations in precipitation but also on annual rainfall amounts. As shown in Fig. 8, annual wet/bulk deposition fluxes of NH_4^+-N and NO_3^--N both showed significantly positive correlations with the corresponding annual VWM concentrations of inorganic N and annual precipitation amount, especially for NH_4^+-N, that more significant was found for precipitation amount than concentration. The measured wet/bulk N deposition rates (average 19.3 kg N ha^{-1} yr^{-1}) were almost twice the earlier average wet deposition value of 9.9 kg N ha^{-1} yr^{-1} for period of 1990-2003 in China (Lü and Tian, 2007). Our results show similar regional patterns and comparable magnitudes to those measured in the 2000s in China as reported by Jia et al. (2014) (~14 kg N ha^{-1} yr^{-1}, wet deposition) and Liu et al. (2013) (~21 kg N ha^{-1} yr^{-1}, bulk deposition).

The NH_4^+-N/NO_3^--N ratio in wet/bulk deposition can be used to indicate the relative contribution of N_r from agricultural and industrial activities to N deposition (Pan et al., 2012; Zhan et al., 2015; Zhu et al., 2015) because the major anthropogenic source of NH_4^+-N in precipitation is NH_3 volatilized from animal excrement and the application of nitrogenous fertilizers in agriculture, while anthropogenic sources of NO_3^--N in precipitation originate from NO_x emitted from fossil fuel combustion in transportation, power plant and factories (Cui et al., 2014). In this study the overall annual average ratio of NH_4^+-N/NO_3^--N in wet/bulk deposition was 1.3 ± 0.5 (standard deviation), with an increasing (but not significant) trend for urban (1.2 ± 0.6), rural (1.3 ± 0.4), and background (1.5 ± 0.4) sites (**Fig. 5b**). Our measured ratio was slightly lower than average values of 1.6 in Europe (Holland et al., 2005) and 1.5 in the United States (Du et al., 2014), and similar to an average value (1.2) reported elsewhere for 2013 in China (Zhu et al., 2015). Based on these findings, we conclude that NH_4^+-N from agricultural sources still dominates wet/bulk N deposition but the contribution has

515 decreased drastically between the 1980s and the 2000s (Liu et al., 2013). Reduced N
516 also contributed more than oxidized N to the total N deposition, and the ratio of
517 reduced to oxidized N deposition overall averaged 1.6 ± 0.7 in dry deposition and 1.4
518 ± 0.4 in the total deposition (**Fig. 5a, c**).
519 The overall mean annual deposition fluxes (wet/bulk plus dry) of NH_x and NO_y for
520 the period 2010-2014 was graded into five levels and plotted on maps showing the
521 spatial distribution of NH_3 and NO_x emissions (**Fig. 9a, b**). The anthropogenic
522 emission data of NH_3 and NO_x for the year 2010 in China were obtained from
523 the **GAINS (Greenhouse Gas and Air Pollution Interactions and Synergies)** model
524 (http://www.iiasa.ac.at/), and emission details for the 33 provinces of China are
525 summarized in **Table S5** of the Supplement. The spatial patterns of estimated NH_x
526 and NO_y deposition compare reasonably well with the regional patterns of NH_3 and
527 NO_x emissions, respectively, even though the emission data were estimated at the
528 province scale. With emission data, N deposition can be used to distinguish regional
529 differences in reactive N_r pollution. Across six regions, significantly positive
530 correlations were found between NH_3 emissions and NH_x deposition fluxes
531 (R^2=0.888, p<0.01) (**Fig. 9c**), and between NO_x emissions and NO_y deposition fluxes
532 (R^2=0.805, p<0.05) (**Fig. 9d**), implying that the N deposition fluxes to the six regions
533 are strongly dependent on the spatial pattern of anthropogenic N_r emissions among
534 the regions. The slopes of the relationships of NH_x vs. NH_3, and NO_y vs. NO_x were
535 0.51 and 0.48, which could be roughly interpreted that NH_x and NO_y deposition
536 fluxes represent about 51% NH_3 and 48% NO_x emissions, respectively.
537 For all Chinese regions except NC we cannot compare our data with other studies
538 because observations for different pollution climate sites in other regions are lacking.
539 For NC, the overall average total N deposition was 56.2 ± 14.8 kg N ha^{-1} yr^{-1}, 13-32%
540 lower than the previously estimated values in Northern China (Pan et al., 2012; Luo et
541 al., 2013). This difference may reflect differences in the numbers of sampling sites,
542 land use type and assumed dry deposition velocities. As expected, our estimated
543 deposition was substantially higher than the results of Lü and Tian (2007), who
544 suggested that the total N deposition ranged from 13 to 20 kg N ha^{-1} yr^{-1} in NC. This
545 is attributed to their omission of many major species (e.g., gaseous NH_3, HNO_3 and
546 particulate N_r) from their data.
547 Compared to dry and wet N deposition fluxes estimated by CASTNET in the United
548 States, EMEP in Europe, and EANET sites in Japan, the average values of dry and

549 wet/bulk deposition in China are much higher (**Table 1**). In addition, on the basis of
550 2001 ensemble-mean modeling results from 21 global chemical transport models (Vet
551 et al., 2014), three global N deposition hotspots were: western Europe (with levels
552 from 20.0 to 28.1 kg N ha^{-1} yr^{-1}), South Asia (Pakistan, India and Bangladesh) from
553 20.0 to 30.6 kg N ha^{-1} yr^{-1} and East Asia from 20 to 38.6 kg N ha^{-1} yr^{-1} in eastern
554 China (the global maximum). Extensive areas of high deposition from 10 to 20 kg N
555 ha^{-1} yr^{-1} appear in the eastern U.S. and southeastern Canada as well as most of central
556 Europe. Small areas with total deposition of N from 10 to 20 kg N ha^{-1} yr^{-1} are present,
557 and very large areas of the continents have deposition from 2 to 10 kg N ha^{-1} yr^{-1}. In
558 contrast, the present study shows a much higher total deposition flux (39.9 kg N
559 ha^{-1} yr^{-1}) at a national scale. In China, the consumption rates of chemical fertilizer and
560 fossil fuel have increased 2.0- and 3.2-fold, respectively, between the 1980s and the
561 2000s (Liu et al., 2013). As a result, the estimated total emission of NH_3 reached 9.8
562 Tg in 2006, contributing approximately 15% and 35% to the global and Asian NH_3
563 emissions (Huang et al., 2012), and NO_x emissions from fossil fuel combustion
564 increased from 1.1 Tg N in 1980 to about 6.0 Tg N in 2010 (Liu et al., 2013). The
565 increasing NO_x and NH_3 emissions in China led to higher atmospheric N deposition
566 than those observed in other regions.
567 According to Endo et al. (2011), the low dry deposition fluxes in CASTNET, EMEP
568 and Japan's EANET network are due at least partly to low concentrations of N_r
569 compounds and/or the omission of dry deposition fluxes of major N_r species (e.g.,
570 NO_2 and NH_3) from the data. Meanwhile, the low wet deposition fluxes at these
571 networks are likely to be a result of the combined effects of low amounts of
572 precipitation and, especially, low atmospheric N_r concentrations. In addition,
573 emissions of nitrogen compounds in other parts of the world are declining. In the U.S.,
574 for example, NO_x emissions from the power sector and mobile sources were reduced
575 by half from 1990 to 2010 (Xing et al., 2013), which explained the declined N
576 deposition fluxes during the period of 1990-2009 observed at 34 paired dry and wet
577 monitoring sites in the eastern US (Sickles II et al., 2015). In Europe, the total NO_x
578 and NH_3 emissions decreased by 31% and 29% from 1990 to 2009 (Torseth et al.,
579 2012). N deposition has decreased or stabilized in the United States and Europe since
580 the late 1980s or early 1990s with the implementation of stricter legislation to reduce
581 emissions (Goulding et al., 1998; Holland et al., 2005). However, wet deposition of
582 ammonia or ammonium, which is not regulated, has increased over recent decades in

583 the U.S. (Du et al., 2014).

584 *4.3 Implications of monitoring N_r concentration and deposition on regional N*
585 *deposition simulation*

586 Our results show that atmospheric concentrations and deposition of N_r in China were
587 high in the 2000s, although the government has made considerable efforts to control
588 environmental pollution by improving air quality in mega cities during and after the
589 2008 Beijing Summer Olympic Games (Wang et al., 2010; Chan and Yao, 2008).
590 Ideally, the spatial distribution of monitoring sites should reflect the gradients in the
591 concentrations and deposition fluxes of atmospheric N_r species. Given the fact that the
592 arithmetic averages used in this study cannot give a completely accurate evaluation of
593 N_r levels for the regions of China due to the limited numbers of monitoring sites and
594 land use types, it is important to develop and improve the quantitative methods for
595 determining N deposition across China.

596 Numerical models are very useful tools to quantify atmospheric N deposition
597 (including both spatial and temporal variations), but a challenge to the modeling
598 approaches is that observations to validate the simulated concentrations and
599 deposition fluxes are often lacking. In our study 43 monitoring sites were selected in a
600 range of land use types to provide more representative regional information on N
601 deposition in China. Although those measurements cannot define all aspects of N
602 deposition across different regions, they add substantially to existing knowledge
603 concerning the spatial patterns and magnitudes of N deposition. The present
604 measurements will be useful for better constraining emission inventories and
605 evaluating simulations from atmospheric chemistry models. In future studies we will
606 use models (e.g., FRAME, Dore et al., 2012) integrated with measurements from our
607 monitoring network to fully address the spatial-temporal variations of atmospheric N
608 deposition and its impacts on natural and semi-natural ecosystems at the
609 regional/national level.

610 *4.4 Uncertainty analysis of the N dry and wet deposition fluxes*

611 The dry deposition fluxes were estimated by combining measured concentrations with
612 modeled V_d. As summarized in **Table S4**, our estimates of dry deposition velocities
613 for different N_r species are generally consistent with previous studies (e.g., Flechard
614 et al., 2011; Pan et al., 2012). Some uncertainties may still exist in the inputs for dry
615 deposition modeling. For example, underlying surface parameters (e.g., surface
616 roughness length and land type) strongly affect dry deposition through their effect on

both deposition velocity and the absorbability of the ground surface to each of the gaseous and particulate N_r species (Loubet et al., 2008). In addition, there is uncertainty in the deposition fluxes for both pNH_4^+ and pNO_3^- in our network, resulting from the difference between the cut-off sizes of particles in the samplers and that defined in the modeled V_d which was calculated for atmospheric $PM_{2.5}$ in GEOS-Chem model. For example, the cut-off sizes of the samples can collect also coarse NO_3^- particles (e.g. calcium nitrate) but should have little effect on NH_4^+ particles (mainly in the fine scale <1 μm) (Tang et al., 2009), resulting in an underestimation of pNO_3^- deposition. Furthermore, NH_3 fluxes over vegetated land are bi-directional and the net direction of this flux is often uncertain. A so-called canopy compensation point was used in previous studies (Sutton et al., 1998) to determine the direction of the NH_3 flux. Since the principle of bi-directional NH_3 exchange was not considered in this study, NH_3 deposition may be overestimated at rural sites with relatively high canopy compensation points (e.g. up to 5 μg N m^{-3}) due to fertilized croplands or vegetation (Sutton et al., 1993).

On the other hand, the total dry deposition flux in this study may be underestimated due to omission of the dry-deposited organic N species in our network and missing HNO_3 data at very few sites as noted earlier (see Sect. 2.2). Organic N species have been found to make an important contribution to the N dry deposition. For example, PAN accounted for 20% of the daytime, summertime NO_y ($NO + NO_2 + HNO_3 + NO_3^- + PAN$) dry deposition at a coniferous forest site (Turnipseed et al., 2006). However, the contribution of PAN and other known atmospheric organic nitrates to total N_r inputs must be minor on an annual time scale, as reported by Flechard et al. (2012). In previous work, dry deposition flux was inferred from atmospheric N_r concentrations and a literature-based annual mean deposition velocity (Shen et al., 2009), or reported by Luo et al. (2013) who did not consider the different dry deposition velocities of various N_r species among different land use types. Clearly, in this study we have greatly improved the estimation of dry deposition, but further work is still required to increase the reliability and accuracy of N dry deposition values.

Since wet/bulk deposition was measured directly, the reported fluxes are considered more accurate than dry deposition fluxes but still some uncertainties exist. On one hand, the estimated fluxes obtained from the open precipitation samplers contain contributions from wet plus unquantifiable dry deposition (including both gases and particles) and therefore likely overestimate actual wet deposition (Cape et al., 2009).

For example, our previous research showed that annual unquantifiable dry deposition (the difference between bulk and wet deposition, approx. 6 kg N ha^{-1} on average) accounted for 20% of bulk N deposition based on observations at three rural sites on the North China Plain (Zhang et al., 2008b). This contribution increased to 39% in urban areas based on a recent measurement (Zhang et al., 2015). On the other hand, dissolved organic N compounds, which have been observed to contribute to be around 25-30% of the total dissolved nitrogen in wet deposition around the world (Jickells et al., 2013) and approximately 28% of the total atmosphere bulk N deposition in China (Zhang et al., 2012b), were not considered in the present study. Their exclusion here would contribute to an underestimation of the total wet N deposition.

Although the NNDMN is the only long-term national deposition network to monitor both N wet/bulk and dry deposition in China till now, large areas of the country and islands do not contain sampling points which may result in missing hotspots or pristine sites of N deposition. The implementation of an adequate monitoring program is also difficult at present in some regions (e.g., northwest China and the Tibetan Plateau). To address this issue, more new monitoring sites, covering regions with both extremely low and high N_r emissions, should be set up in the NNDMN in future work.

Conclusions

In this paper, we systematically reported large spatial variations in annual mean concentrations (1.3-47.0 μg N m^{-3}), dry (1.1 to 52.2 kg N ha^{-1} yr^{-1}), wet/bulk (1.5-32.5 kg N ha^{-1} yr^{-1}) and total (2.9 to 83.3 kg N ha^{-1} yr^{-1}) deposition fluxes of atmospheric N_r species across the forty-three monitoring sites in China. On a regional/national basis, the annual mean concentrations and deposition fluxes of N_r species ranked by the same order of urban > rural > background sites and NC > SE > SW > NE > NW > TP, reflecting the impact of varying anthropogenic N_r emissions in different land use types and/or regions.

Dry deposition fluxes of N_r species on average contributed 52% of the total N deposition (39.9 kg N ha^{-1} yr^{-1}) across all sites, indicating the importance of dry deposition monitoring for a complete N deposition assessment at the national scale. Annual average ratios of reduced N/oxidized N in dry, wet/bulk and total deposition were 1.6, 1.3 and 1.4, respectively, suggesting that reduced N, mainly from

agricultural sources, still dominates dry, wet/bulk, and total N deposition in China.

Our work represents the first effort to investigate both dry and wet/bulk N deposition simultaneously, based on a nationwide monitoring network in China. We consider this unique dataset important not only for informing policy-makers about the abatement of pollutant emissions and ecosystem protection but also validating model estimations of N deposition at the regional/national scale. For better understanding atmospheric N deposition fluxes in China, further studies in the future are still required at least the two following aspects: (1) to cover more representative monitoring sites; (2) to improve the dry deposition velocity estimates of various N_r species using a single-point dry deposition model as for CASTNET.

Acknowledgments

This study was supported by the Chinese National Basic Research Program (2014CB954202), the China Funds for Distinguished Young Scholars of NSFC (40425007), and the National Natural Science Foundation of China (31121062, 41321064 and 41405144). The authors thank all technicians at monitoring sites in NNDMN.

References

Bey, I., Jacob, D. J., Yantosca, R. M., Logan, J. A., Field, B. D., Fiore, A. M., Li, Q., Liu, H., Mickley, L. J., and Schultz, M. G.: Global modeling of tropospheric chemistry with assimilated meteorology: Model description and evaluation, J. Geophys. Res., 106(D19), 23,073 –23,096, 2001.

Behera, S. N., Sharma, M., Aneja, V. P., and Balasubramanian, R.: Ammonia in the atmosphere: a review on emission sources, atmospheric chemistry and deposition on terrestrial bodies, Environ. Sci. Pollut. Res., 20, 8092–8131, doi:10.1007/s11356-013-2051-9, 2013.

Cape, J.N., Van Dijk, N., and Tang, Y.S.: Measurement of dry deposition to bulk collectors using a novel flushing sampler. J. Environ. Monit., 11, 353-358, doi: 10.1039/B813812E, 2009.

Chan, C.K. and Yao, X.H.: Air pollution in mega cities in China, Atmos. Environ., 42,

713 1–42, doi: 10.1016/j.atmosenv.2007.09.003, 2008.
714 Chen, D., Wang, Y. X., McElroy, M. B., He, K., Yantosca, R. M., and Le Sager, P.:
715 Regional CO pollution in China simulated by high-resolution nested-grid
716 GEOS-Chem model, Atmos. Chem. Phys., 11, 3825-3839, 2009.
717 Chen, X. Y. and Mulder, J.: Atmospheric deposition of nitrogen at five subtropical
718 forested sites in South China, Sci. Total Environ., 378, 317–330, doi:
719 10.1016/j.scitotenv.2007.02.028, 2007.
720 Clark, C. M. and Tilman, D.: Loss of plant species after chronic low-level nitrogen
721 deposition to prairie grasslands, Nature, 451, 712–715, doi:10.1038/nature06503,
722 2008.
723 Clarke, J. F., Edgerton, E. S., and Martin, B. E.: Dry deposition calculations for the
724 Clean Air Status and Trends Network, Atmos. Environ., 31, 3667-3678, 1997.
725 CSY (China Statistical Yearbook), 2007-2014. Available at: http://www.stats.gov.cn.
726 Cui, J., Zhou, J., Peng, Y., He, Y. Q., Yang, H., Mao, J. D., Zhang, M. L., Wang, Y. H.,
727 and Wang, S. W.: Atmospheric wet deposition of nitrogen and sulfur in the
728 agroecosystem in developing and developed areas of Southeastern China, Atmos.
729 Environ., 89, 102–108, doi:10.1016/j.atmosenv.2014.02.007, 2014.
730 Dentener, F., Drevet, J., Lamarque, J. F., Bey, L., Eickhout, B., Fiore, A.
731 M. Hauglustaine, D., Horowitz, L. W., Krol, M., and Kulshrestha, U. C .:
732 Nitrogen and sulfur deposition on regional and global scales: a multimodel
733 evaluation, Global Biogeochemical Cy., 20, GB4003, doi: 10.1029/2005GB002672,
734 2006.
735 Dore, A.J., Kryza, M., Hall, J. Hallsworth, S., Keller, V., Vieno, M. and Sutton, M.A.:
736 The influence of model grid resolution on estimation of national scale nitrogen
737 deposition and exceedance of critical loads, Biogeosciences, 9, 1597-1609, 2012.
738 Du, E. Z., Vries, W. D., Galloway, J. N., Hu, X. Y., and Fang, J. Y.: Changes in wet
739 nitrogen deposition in the United States between 1985 and 2012, Environ. Res.
740 Lett., 9, 095004, doi:10.1088/1748-9326/9/9/095004, 2014.
741 EEA: Air Quality in Europe-2011 Report. Technical Report 12/2011. EEA,
742 Kopenhagen, 2011.

743 Ellis, R. A., Jacob, D. J., Sulprizio, M. P., Zhang, L., Holmes, C. D., Schichtel, B. A.,
744 Blett, T., Porter, E., Pardo, L. H., and Lynch, J. A.: Present and future nitrogen
745 deposition to national parks in the United States: critical load exceedances, Atmos.
746 Chem. Phys., 13, 9083-9095, doi:10.5194/acp-13-9083-2013, 2013.
747 Endo, T., Yagoh, H., Sato, K., Matsuda, K., Hayashi, K., Noguchi, I., and Sawada, K.:
748 Regional characteristics of dry deposition of sulfur and nitrogen compounds at
749 EANET sites in Japan from 2003 to 2008, Atmos. Environ., 45,
750 1259–1267,doi:10.1016/j.atmosenv.2010.12.003, 2010.
751 Erisman, J. W., Vermeulen, A., Hensen, A., Flechard, C., Dammgen, U., Fowler, D.,
752 Sutton, M., Grunhage, L., and Tuovinen, J.P.: Monitoring and modelling of
753 biosphere/atmosphere exchange of gases and aerosols in Europe, Environ. Pollut.,
754 133, 403–413, doi:10.1016/j.envpol.2004.07.004, 2005.
755 Flechard, C. R., Nemitz, E., Smith, R. I., Fowler, D., Vermeulen, A. T., Bleeker, A.,
756 Erisman, J. W., Simpson, D., Zhang, L., Tang, Y. S., and Sutton, M. A.: Dry
757 deposition of reactive nitrogen to European ecosystems: a comparison of inferential
758 models across the NitroEurope network, Atmos. Chem. Phys., 11,
759 2703–2728,doi:10.5194/acp-11-2703-2011, 2011.
760 Fowler, D., Coyle, M., Skiba, U., Sutton, M. A., Cape, J. N., Reis, S., Sheppard, L. J.,
761 Jenkins, A., Grizzetti, B., Galloway, J. N., Vitousek, P., Leach, A., Bouwman, A. F.,
762 Butterbach-Bahl, K., Dentener, F., Stevenson, D., Amann, M., and Voss, M.: The
763 global nitrogen cycle in the twenty-first century, Phil. Trans. R. Soc. B, 368,
764 20130164, doi:10.1098/rstb.2013.0164, 2013.
765 Galloway, J. N., Dentener, F. J., Capone, D. G., Boyer, E. W., Howarth, R. W.,
766 Seitzinger, S. P., Asner, G. P., Cleveland, C. C., Green, P. A., Holland, E. A., Karl,
767 D. M., Michaels, A. F., Porter, J. H., Townsend, A. R., and Vorosmarty, C. J.:
768 Nitrogen cycles: past, present, and future, Biogeochem., 70, 153–226, 2004.
769 Galloway, J. N., Townsend, A. R., Erisman, J. W., Bekunda, M., Cai, Z., Freney, J. R.,
770 Martinelli, L. A., Seitzinger, S. P., and Sutton, M. A.: Transformation of the
771 Nitrogen Cycle: Recent trends, questions, and potential solutions, Science, 320,
772 889–892, 2008.

773 Galloway, J. N., Leach, A. M., Bleeker, A., and Erisman, J. W.: A chronology of
774 human understanding of the nitrogen cycle, Phil. Trans. R. Soc. B, 368, 20130120,
775 doi:10.1098/rstb.2013.0120, 2013.
776 Goulding, K. W. T., Bailey, N. J., Bradbury, N. J., Hargreaves, P., Howe, M., Murphy,
777 D. V., Poulton, P. R., and Willison, T. W.: Nitrogen deposition and its contribution
778 to nitrogen cycling and associated soil processes, New Phytol., 139, 49–58, 1998.
779 Gu, B. J., Ge, Y., Ren, Y., Xu, B., Luo, W. D., Jiang, H., Gu, B. H., and Chang, J.:
780 Atmospheric reactive nitrogen in China: Sources, recent trends, and damage costs,
781 Environ. Sci. Technol., 46, 9240–9247, doi:10.1021/es301446g, 2012.
782 Gu, B. J., Sutton, M. A., Chang, S. X., Ge, Y., and Jie, C.: Agricultural ammonia
783 emissions contribute to China's urban air pollution, Front. Ecol. Environ., 12,
784 265–266, doi:10.1890/14.WB.007, 2014.
785 Holland, E. A., Braswell, B. H., Sulzman, J., and Lamarque, J. F.: Nitrogen deposition
786 onto the United States and Western Europe: synthesis of observations and models,
787 Ecol. Appl., 15, 38–57, 2005.
788 Hu, H., Yang, Q., Lu, X., Wang, W., Wang, S., and Fan, M.: Air pollution and control
789 in different areas of China. Crit. Rev. Environ. Sci. Technol., 40, 452–518,
790 doi:10.1080/10643380802451946, 2010.
791 Huang, X., Song, Y., Li, M. M., Li, J. F., Huo, Q., Cai, X. H., Zhu, T., Hu, M., and
792 Zhang, H. S.: A high-resolution ammonia emission inventory in China, Global
793 Biogeochem. Cy., 26, GB1030, doi:10.1029/2011GB004161, 2012.
794 Huang, Y. L., Lu, X. X., and Chen, K.: Wet atmospheric deposition of nitrogen: 20
795 years measurement in Shenzhen City, China, Environ. Monit. Assess., 185, 113–
796 122, doi: 10.1007/s10661-012-2537-9, 2013.
797 Jia, Y. L., Yu, G. R., He, N. P., Zhan, X. Y., Fang, H. J., Sheng, W. P., Zuo, Y., Zhang,
798 D. Y., and Wang, Q. F.: Spatial and decadal variations in inorganic nitrogen wet
799 deposition in China induced by human activity. Sci. Rep., 4, 3763, doi:
800 10.1038/srep03763, 2014.
801 Jickells, T., Baker, A. R., Cape, J. N., Cornell, S.E., and Nemitz, E.: The cycling of
802 organic nitrogen through the atmosphere. Philos. Trans. R. Soc. B 368, 20130115,

803 doi:org/10.1098/rstb.2013.0115, 2013.
804 Li, Y. E. and Lin, E. D.: Emissions of N_2O, NH_3 and NO_x from fuel combustion,
805 industrial processes and the agricultural sectors in China. Nutr. Cycl. Agroecosys.,
806 57, 99–106, 2000.
807 Liu, X. J., Song, L., He, C. E., and Zhang, F. S.: Nitrogen deposition as an important
808 nutrient from the environment and its impact on ecosystems in China, J. Arid Land,
809 2, 137–143, 2010.
810 Liu, X. J., Duan, L., Mo, J. M., Du, E., Shen, J. L., Lu, X. K., Zhang, Y., Zhou, X. B.,
811 He, C. E., and Zhang, F. S.: Nitrogen deposition and its ecological impact in China:
812 An overview, Environ. Pollut., 159, 2251–2264, doi:10.1016/j.envpol.2010.08.002,
813 2011.
814 Liu, X. J., Zhang, Y., Han, W. X., Tang, A., Shen, J. L., Cui, Z. L., Vitousek, P.,
815 Erisman, J. W., Goulding, K., Christie, P., Fangmeier, A., and Zhang, F. S.:
816 Enhanced nitrogen deposition over China, Nature, 494, 459–462,
817 doi:10.1038/nature11917, 2013.
818 Liu, X. J., Xu, W., Pan, Y. P., and Du, E. Z.: Liu et al. suspect that Zhu et al. (2015)
819 may have underestimated dissolved organic nitrogen (N) but overestimated total
820 particulate N in wet deposition in China, Sci. Total Environ., 520, 300–301,
821 doi.org/10.1016/j.scitotenv.2015.03.004, 2015.
822 Loubet, B., Asman, W. A. H., Theobald, M. R., Hertel, O., Tang, S. Y., Robin, P.,
823 Hassouna, M., Dämmgen, U., Genermont, S., Cellier, P., and Sutton, M. A.:
824 Ammonia deposition near hot spots: processes, models and monitoring methods. In:
825 Sutton MA, Reis S, Baker SMH, editors. Atmospheric ammonia: detecting
826 emission changes and environmental impacts. Netherlands: Springer;
827 205-251.,2008.
828 Lü, C. Q. and Tian, H. Q.: Spatial and temporal patterns of nitrogen deposition in
829 China: Synthesis of observational data, J. Geophys. Res., 112, D22S05,
830 doi:10.1029/2006JD007990, 2007.
831 Lü, C. Q. and Tian, H. Q.: Half-century nitrogen deposition increase across China: A
832 gridded time-series data set for regional environmental assessments. Atmos.

Environ., 97, 68-74, 2014.

Luo, X. S., Liu, P., Tang, A. H., Liu, J. Y., Zong, X. Y., Zhang, Q., Kou, C. L., Zhang, L. J., Fowler, D., Fangmeier, A., Christie, P., Zhang, F. S., and Liu, X. J.: An evaluation of atmospheric Nr pollution and deposition in North China after the Beijing Olympics, Atmos. Environ., 74, 209–216, doi:10.1016/j.atmosenv.2013.03.054, 2013.

Maston, P., Lohse, K. A., and Hall, S. J.: The globalization of nitrogen deposition: Consequences for terrestrial ecosystems, Ambio, 31, 113–119, 2002.

MEPC (Ministry of Environmental Protection of the People's Republic of China): China's environment and data center. www.zhb.gov.cn/. Viewed 23 April 2014, 2014

Pan, Y. P., Wang, Y. S., Tang, G. Q., and Wu, D.: Wet and dry deposition of atmospheric nitrogen at ten sites in Northern China. Atmos. Chem. Phys., 12, 6515-6535, doi:10.5194/acp-12-6515-2012, 2012.

Reche, C., Viana, M., Pandolfi, M., Alastuey, A., Moreno, T., Amato, F., Ripoll, A., and Querol, X.: Urban NH_3 levels and sources in a Mediterranean environment. Atmos. Environ., 57:153–164, doi:10.1016/j.atmosenv.2012.04.021, 2012.

Richter, D. D., Burrows, J. P., N Nüß, H., Granier, C., and Niemeier, U.: Increase in tropospheric nitrogen dioxide over China observed from space, Nature 437, 129–132, 2005.

Seinfeld, J. and Pandis, S.: Atmospheric Chemistry and Physics: From Air Pollution to Climate Change, John Wiley and Sons, 2nd Edition, 1203 pp., 2006.

Schwede, D., Zhang, L., Vet, R., and Lear, G.: An intercomparison of the deposition models used in the CASTNET and CAPMoN networks, Atmos. Environ., 45, 1337–1346, doi:10.1016/j.atmosenv.2010.11.050, 2011.

Shen, J. L., Tang, A. H., Liu, X. J., Fangmeier, A., Goulding, K. T. W., and Zhang, F. S.: High concentrations and dry deposition of reactive nitrogen species at two sites in the North China Plain, Environ. Pollut., 157, 3106–3113, doi:10.1016/j.envpol.2009.05.016, 2009.

Simpson, D., Fagerli, H., Jonson, J.E., Tsyro, S., Wind, P., and Tuovinen, J. P.:

Trans-boundary Acidification and Eutrophication and Ground Level Ozone in Europe: Unified EMEP Model Description, EMEP Status Report 1/2003 Part I, EMEP/MSC-W Report, The Norwegian Meteorological Institute, Oslo, Norway, 2003.

Skeffington, R. A. and Hill, T. J.: The effects of a changing pollution climate on throughfall deposition and cycling in a forested area in southern England, Sci. Total Environ., 434 , 28–38, doi:10.1016/j.scitotenv.2011.12.038, 2012.

Sickles, J. E. and Shadwick, D. S.: Air quality and atmospheric deposition in the eastern US: 20 years of change, Atmos. Chem. Phys., 15, 173–197, doi: 10.5194/acp-15-173-2015, 2015.

Sutton, M.A., Pitcairn, C.E.R., and Fowler, D.: The exchange of ammonia between the atmosphere and plant communities. Adv. Ecol. Res., 24, 301-393, doi:10.1016/S0065-2504(08)60045-8, 1993.

Sutton, M. A., Burkhardt, J. K., Guerin, D., Nemitz, E., and Fowler, D.: Development of resistance models to describe measurements of bi-directional ammonia surface-atmosphere exchange, Atmos. Environ., 32, 473–480, doi:10.1016/S1352-2310(97)00164-7,1998.

Sutton, M. A., Tang, Y. S., Miners, B., and Fowler, D.: A new diffusion denuder system for long-term, regional monitoring of atmospheric ammonia and ammonium, Water Air Soil Poll. Focus, 1, 145–156, 2001.

Tang, Y. S., Simmons, I., van Dijk, N., Di Marco, C., Nemitz, E., Dammgen, U., Gilke, K., Djuricic, V., Vidic, S., Gliha, Z.: European scale application of atmospheric reactive nitrogen measurements in a low-cost approach to infer dry deposition fluxes. Agr. Ecosyst. Environ., 133, 183–195, doi: 10.1016/j.agee.2009.04.027, 2009.

Torseth, K., Aas, W., Breivik, K., Fjaeraa, A. M., Fiebig, M., Hjellbrekke, A. G., Myhre, C. L., Solberg, S., Yttri, K. E.: Introduction to the European Monitoring and Evaluation Programme (EMEP) and observed atmospheric composition change during 1972–2009, Atmos. Chem. Phys., 12, 5447–5481, doi: 10.5194/acp-12-5447-2012, 2012.

Vitousek, P. M., Aber, J. D., Howarth, R. W., Likens, G. E., Matson, P. A., Schindler, D. W., Schlesinger, W. H., and Tilman, D. G.: Human alteration of the global nitrogen cycle: Sources and consequences, Ecol. Appl., 7, 737–750, 1997.

Vet, R., Artz, R. S., Carou, S., Shaw, M., Ro, C-U., Aas, W., Baker, A., and 14 authors: A global assessment of precipitation chemistry and deposition of sulfur, nitrogen, sea salt, base cations, organic acids, acidity and pH, and phosphorus, Atmos. Environ., 93, 3–100, doi:10.1016/j.atmosenv.2013.10.060, 2014.

Wang, S. X., Xing, J., Zhao, B., Jang, C., and Hao, J. M.: Effectiveness of national air pollution control policies on the air quality in metropolitan areas of China, J. Environ. Sci., 26, 13–22, doi: 10.1016/S1001-0742(13)60381-2, 2014.

Wang, T., Nie, W., Gao, J., Xue, L. K., Gao, X. M., Wang, X. F., Qiu, J., Poon, C. N., Meinardi, S., Blake, D., Wang, S. L., Ding, A. J., Chai, F. H., Zhang, Q. Z., and Wang, W. X.: Air quality during the 2008 Beijing Olympics: secondary pollutants and regional impact, Atmos. Chem. Phys., 16, 7603–7615, doi:10.5194/acp-10-7603-2010, 2010.

Wesely, M. L.: Parameterization of surface resistances to gaseous dry deposition in regional-scale numerical-models, Atmos. Environ., 23, 1293-1304, 1989.

Xing, J., Pleim, J., Mathur, R., Pouliot, G., Hogrefe, C., Gan, C. M., Wei, C.: Historical gaseous and primary aerosol emissions in the United States from 1990 to 2010, Atmos. Chem. Phys., 13, 7531–7549, doi: 10.5194/acp-13-7531-2013, 2013.

Yu, W. T., Jiang, C. M., Ma, Q., Xu, Y. G., Zou, H., and Zhang, S. C.: Observation of the nitrogen deposition in the lower Liaohe River Plain, Northeast China and assessing its ecological risk, Atmos. Res., 101, 460–468, doi:10.1016/j.atmosres.2011.04.011, 2011.

Zhan, X., Yu, G., He, N., Jia, B., Zhou, M., Wang, C., Zhang, J., Zhao, G., Wang, S., Liu, Y., and Yan, J.: Inorganic nitrogen wet deposition: Evidence from the North-South Transect of Eastern China, Environ. Pollut., 204, 1–8, doi: 10.1016/j.envpol.2015.03.016, 2015.

Zhang, F. S., Wang, J. Q., Zhang, W. F., Cui, Z. L., Ma, W. Q., Chen, X. P., and Jiang, R. F.: Nutrient use efficiency of major cereal crops in China and measures for

improvement. Acta. Pedologia Sinica, 45, 915–924, 2008a (in Chinese with English abstract).

Zhang, G. Z., Pan, Y. P., Tian, S. L., Cheng, M. T., Xie, Y. Z., Wang, H., and Wang, Y. S.: Limitations of passive sampling technique of rainfall chemistry and wet deposition flux characterization. Res. Environ. Sci., 28, 684-690, doi:10. 13198/j.issn.1001-6929.2015.05.03, 2015.

Zhang, L., Jacob, D. J., Knipping, E. M., Kumar, N., Munger, J. W., Carouge, C. C., van Donkelaar, A., Wang, Y. X., and Chen, D.: Nitrogen Deposition to the United States: Distribution, Sources, and Processes, Atmos. Chem. Phys., 12, 4539-4554, doi:10.5194/acp-12-4539-2012, 2012a.

Zhang, L. M., Gong, S. L., Padro, J., and Barrie, L.: A size-segregated particle dry deposition scheme for an atmospheric aerosol module, Atmos. Environ., 35 (3), 549-560, doi:10.1016/s1352-2310(00)00326-5, 2001.

Zhang, Y., Liu, X. J., Fangmeier, A., Goulding, K. T. W., and Zhang, F. S.: Nitrogen inputs and isotopes in precipitation in the North China Plain, Atmos. Environ., 42, 1436–1448, doi:10.1016/j.atmosenv.2007.11.002, 2008b.

Zhang, Y., Dore, A. J., Ma, L., Liu, X. J., Ma, W. Q., Cape, J. N., and Zhang, F. S.: Agricultural ammonia emissions inventory and spatial distribution in the North China Plain, Environ. Pollut., 158, 490–501, doi:10.1016/j.envpol.2009.08.033, 2010.

Zhang, Y., Song, L., Liu, X. J., Li, W. Q., Lü, S. H., Zheng, L. X., Bai, Z. C., Cui, G.Y., and Zhang, F. S.: Atmospheric organic nitrogen deposition in China. Atmos. Environ., 46, 195–204, doi:10.1016/j.atmosenv.2011.09.080, 2012b.Zhao, Y. H., Zhang, L., Pan, Y. P., Wang, Y. S., Paulot, F., and Henze, D. K.: Atmospheric nitrogen deposition to the northwestern Pacific: seasonal variation and source attribution, Atmos. Chem. Phys. Discuss., 15, 13657-13703, doi:10.5194/acpd-15-13657-2015, 2015.

Zhu, J. X., He, N. P., Wang, Q. F., Yan, G. F., Wen, D., Yu, G. R., and Jia, Y. L.: The composition, spatial patterns, and influencing factors of atmospheric wet nitrogen deposition in Chinese terrestrial ecosystems. Sci. Total Environ., 511, 777-785,

953 doi:org/10.1016/j.scitotenv.2014.12.038, 2015.

954 **Figure captions**

955 **Fig. 1**. Geographical distribution of the forty-three monitoring sites in China.

956 **Fig. 2**. Annual mean concentrations of N_r compounds in air (a) and volume-weighted
957 concentrations of inorganic nitrogen species in precipitation (b) at all monitoring sites.
958 U, R, and B denote urban, rural, and background sites, respectively. TP denotes the
959 Tibetan Plateau.

960 **Fig. 3**. Annual mean concentrations of (a) NH_3; (b) NO_2; (c) HNO_3; (d) pNH_4^+; (e)
961 pNO_3^-; and (f) Total N_r: sum of all measured N_r in air and volume-weighted
962 concentrations of NH_4^+ (g); NO_3^- (h) and Total inorganic N (TIN): sum of NH_4^+ and
963 NO_3^- (i) in precipitation at different land use types in six regions. The number of sites
964 with the same land use type in each region can be found in Table S1 in the
965 Supplement. The error bars are the standard errors of means.

966 **Fig. 4**. Annual mean concentrations and deposition fluxes of N_r compounds at
967 different land use types across China: concentrations in air (a); volume-weighted
968 concentrations in precipitation (b); dry N deposition fluxes (c); wet/bulk N deposition
969 fluxes (d). The number of sites with the same land use type can be found in Table S1
970 in the Supplement. The error bars are the standard errors of means.

971 **Fig. 5**. Annual deposition flux of various N_r species at the forty-three selected sites in
972 China: (a) dry deposition flux; (b) wet/bulk deposition flux; (c) total deposition flux.
973 Yellow dots denote ratios of reduced N to oxidized N in dry deposition (a), NH_4^+-N
974 to NO_3^--N in wet/bulk deposition (b) and/or reduced N to oxidized N in total
975 deposition (c) at all sampling sites. U, R, and B denote urban, rural, and background
976 sites, respectively. TP denotes the Tibetan Plateau.

977 **Fig. 6**. Dry N deposition fluxes of (a) NH_3; (b) NO_2; (c) HNO_3; (d) pNH_4^+; (e) pNO_3^-;
978 and (f) Total N_r: sum of all measured N_r in dry and wet/bulk N deposition fluxes of
979 NH_4^+ (g); NO_3^- (h) and Total inorganic N (TIN): sum of NH_4^+ and NO_3^- (i) at
980 different land use types in the six regions. The number of sites with the same land use
981 type in each region can be found in Table S1 in the Supplement. Error bars are
982 standard errors of means.

983 **Fig. 7**. Contribution of different pathways (dry-deposited N=gaseous N+ particulate N,

wet/bulk-deposited N=precipitation N) to the estimated total N deposition in the six regions: (a) NC: north China; (b) NE: northeast China; (c) NW: northwest China; (d) SE: southeast China; (e) SW: southwest China; (f) TP: Tibetan Plateau.

Fig. 8. Correlations between annual wet/bulk NH_4^+-N deposition and annual volume-weighted concentration of NH_4^+-N (a) and annual precipitation (b); between annual wet/bulk NO_3^--N deposition and annual volume-weighted concentration of NO_3^--N (c) and annual precipitation (d).

Fig. 9. Spatial variation of atmospheric N deposition flux with emission distribution in China: (a) NH_3 emission *vs.* NH_x deposition; (b) NO_x emission vs. NO_y deposition; (c) relationship of NH_x deposition *vs.* NH_3 emission; (d) relationship of NO_y deposition *vs.* NO_x emission.

1014 **Figure 1**

1015

Figure 2

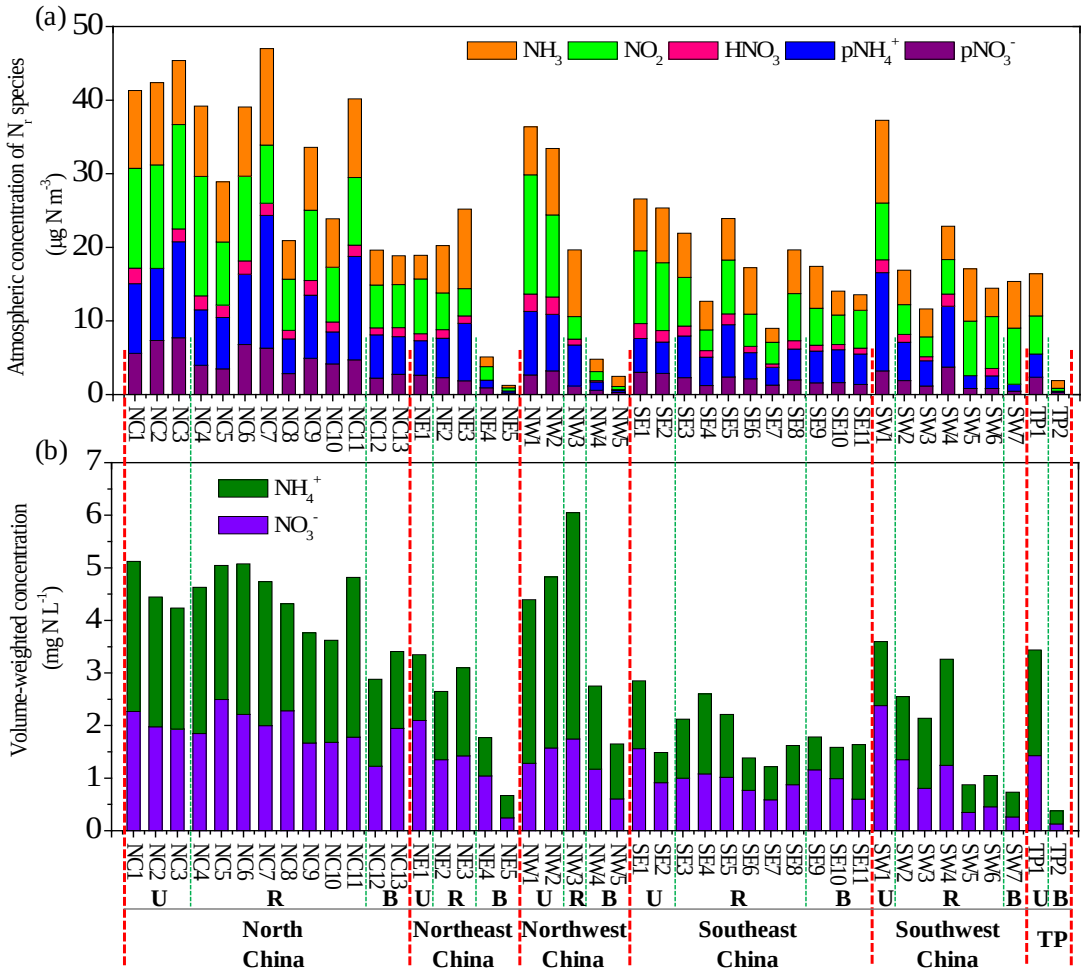
(a)
Atmospheric concentration of N_r species ($\mu g\ N\ m^{-3}$)
NH_3
NO_2
HNO_3
pNH_4^+
pNO_3^-
(b)
Volume-weighted concentration ($mg\ N\ L^{-1}$)
NH_4^+
NO_3^-
NC1 NC2 NC3 NC4 NC5 NC6 NC7 NC8 NC9 NC10 NC11 NC12 NC13 NE1 NE2 NE3 NE4 NE5 NW1 NW2 NW3 NW4 NW5 SE1 SE2 SE3 SE4 SE5 SE6 SE7 SE8 SE9 SE10 SE11 SW1 SW2 SW3 SW4 SW5 SW6 SW7 TP1 TP2
U R B U R B U R B U R B U R B U R B
North China
Northeast China
Northwest China
Southeast China
Southwest China
TP

Figure 3

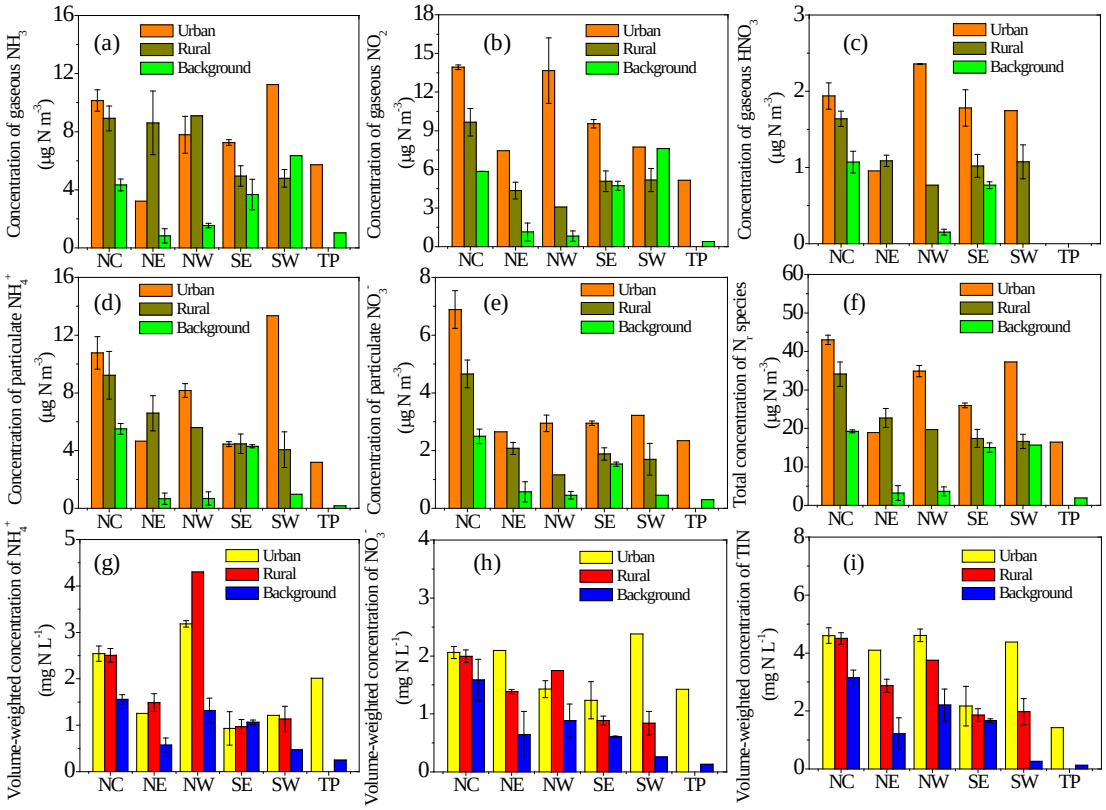
(a)
Urban
Rural
Background
Concentration of gaseous NH_3 ($\mu g\ N\ m^{-3}$)
(b)
Concentration of gaseous NO_2 ($\mu g\ N\ m^{-3}$)
(c)
Concentration of gaseous HNO_3 ($\mu g\ N\ m^{-3}$)
(d)
Concentration of particulate NH_4^+ ($\mu g\ N\ m^{-3}$)
(e)
Concentration of particulate NO_3^- ($\mu g\ N\ m^{-3}$)
(f)
Total concentration of N_r species ($\mu g\ N\ m^{-3}$)
(g)
Volume-weighted concentration of NH_4^+ ($mg\ N\ L^{-1}$)
(h)
Volume-weighted concentration of NO_3^- ($mg\ N\ L^{-1}$)
(i)
Volume-weighted concentration of TIN ($mg\ N\ L^{-1}$)
NC
NE
NW
SE
SW
TP

Figure 4

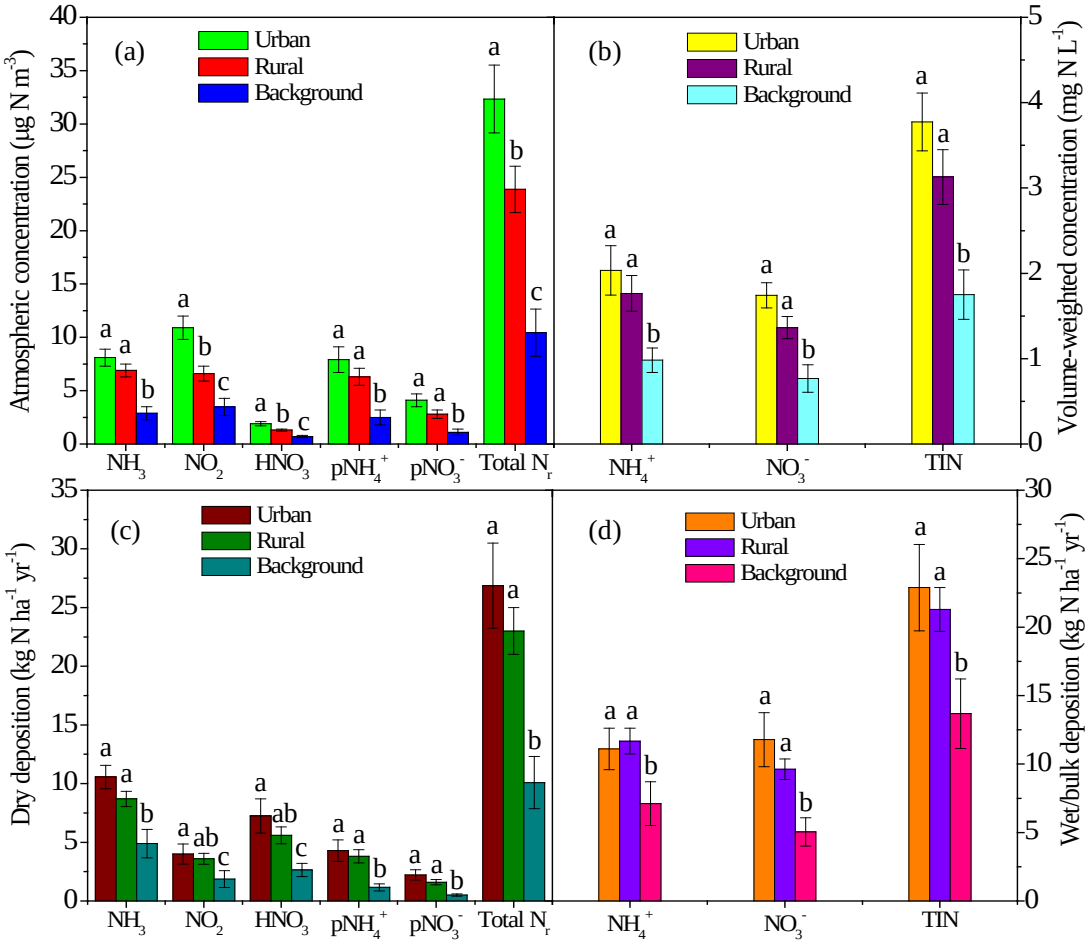
(a)
Urban
Rural
Background
Atmospheric concentration (μg N m-3)
NH3
NO2
HNO3
pNH4+
pNO3-
Total Nr
(b)
Urban
Rural
Background
Volume-weighted concentration (mg N L-1)
NH4+
NO3-
TIN
(c)
Urban
Rural
Background
Dry deposition (kg N ha-1 yr-1)
(d)
Urban
Rural
Background
Wet/bulk deposition (kg N ha-1 yr-1)

Figure 5

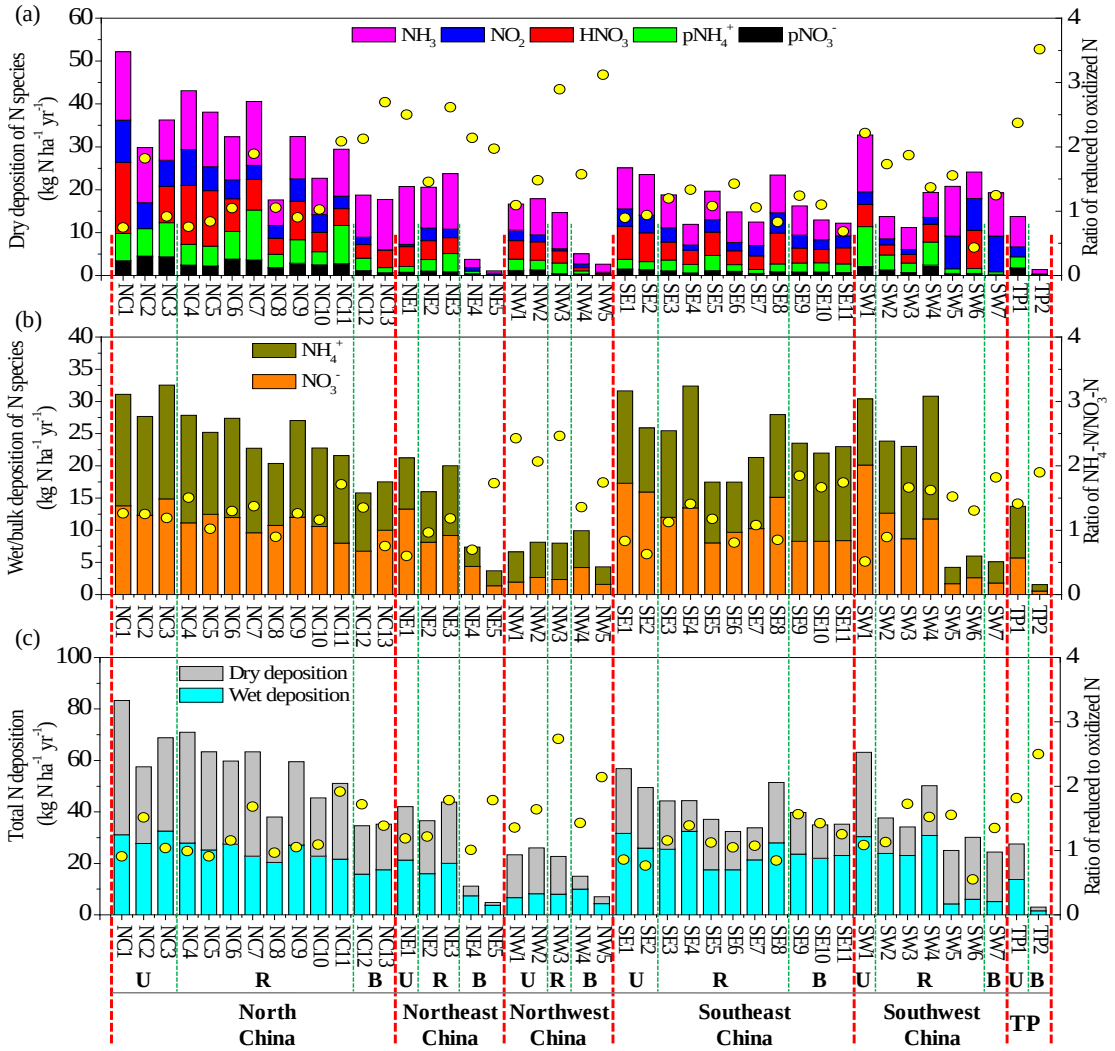
(a)
NH3
NO2
HNO3
pNH4+
pNO3-
Dry deposition of N species (kg N ha-1 yr-1)
Ratio of reduced to oxidized N
(b)
NH4+
NO3-
Wet/bulk deposition of N species (kg N ha-1 yr-1)
Ratio of NH4+-N/NO3--N
(c)
Dry deposition
Wet deposition
Total N deposition (kg N ha-1 yr-1)
Ratio of reduced to oxidized N
NC1 NC2 NC3 NC4 NC5 NC6 NC7 NC8 NC9 NC10 NC11 NC12 NC13 NE1 NE2 NE3 NE4 NE5 NW1 NW2 NW3 NW4 NW5 SE1 SE2 SE3 SE4 SE5 SE6 SE7 SE8 SE9 SE10 SE11 SW1 SW2 SW3 SW4 SW5 SW6 SW7 TP1 TP2
U R B U R B U R B U R B U R B
North China
Northeast China
Northwest China
Southeast China
Southwest China
TP

Figure 6

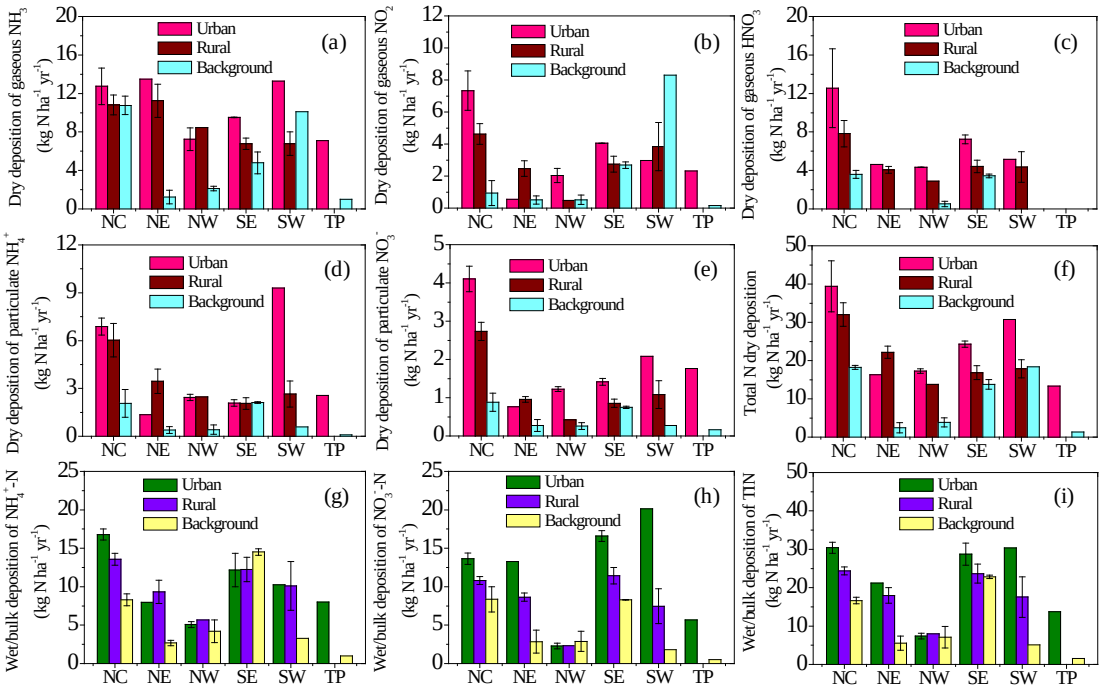
(a)
Dry deposition of gaseous NH_3 (kg N ha^{-1} yr^{-1})
(b)
Dry deposition of gaseous NO_2 (kg N ha^{-1} yr^{-1})
(c)
Dry deposition of gaseous HNO_3 (kg N ha^{-1} yr^{-1})
(d)
Dry deposition of particulate NH_4^+ (kg N ha^{-1} yr^{-1})
(e)
Dry deposition of particulate NO_3^- (kg N ha^{-1} yr^{-1})
(f)
Total N dry deposition (kg N ha^{-1} yr^{-1})
(g)
Wet/bulk deposition of NH_4^+-N (kg N ha^{-1} yr^{-1})
(h)
Wet/bulk deposition of NO_3^--N (kg N ha^{-1} yr^{-1})
(i)
Wet/bulk deposition of TIN (kg N ha^{-1} yr^{-1})
Urban
Rural
Background
NC
NE
NW
SE
SW
TP

Figure 7

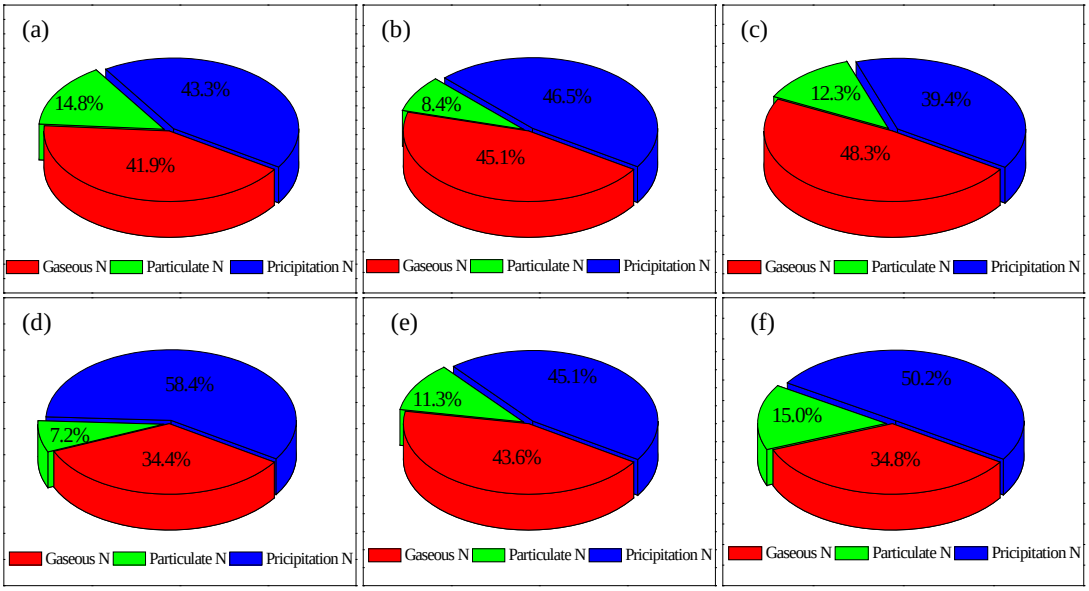
(a)
14.8%
43.3%
41.9%
Gaseous N
Particulate N
Pricipitation N
(b)
8.4%
46.5%
45.1%
Gaseous N
Particulate N
Pricipitation N
(c)
12.3%
39.4%
48.3%
Gaseous N
Particulate N
Pricipitation N
(d)
58.4%
7.2%
34.4%
Gaseous N
Particulate N
Pricipitation N
(e)
45.1%
11.3%
43.6%
Gaseous N
Particulate N
Pricipitation N
(f)
50.2%
15.0%
34.8%
Gaseous N
Particulate N
Pricipitation N

Figure 8

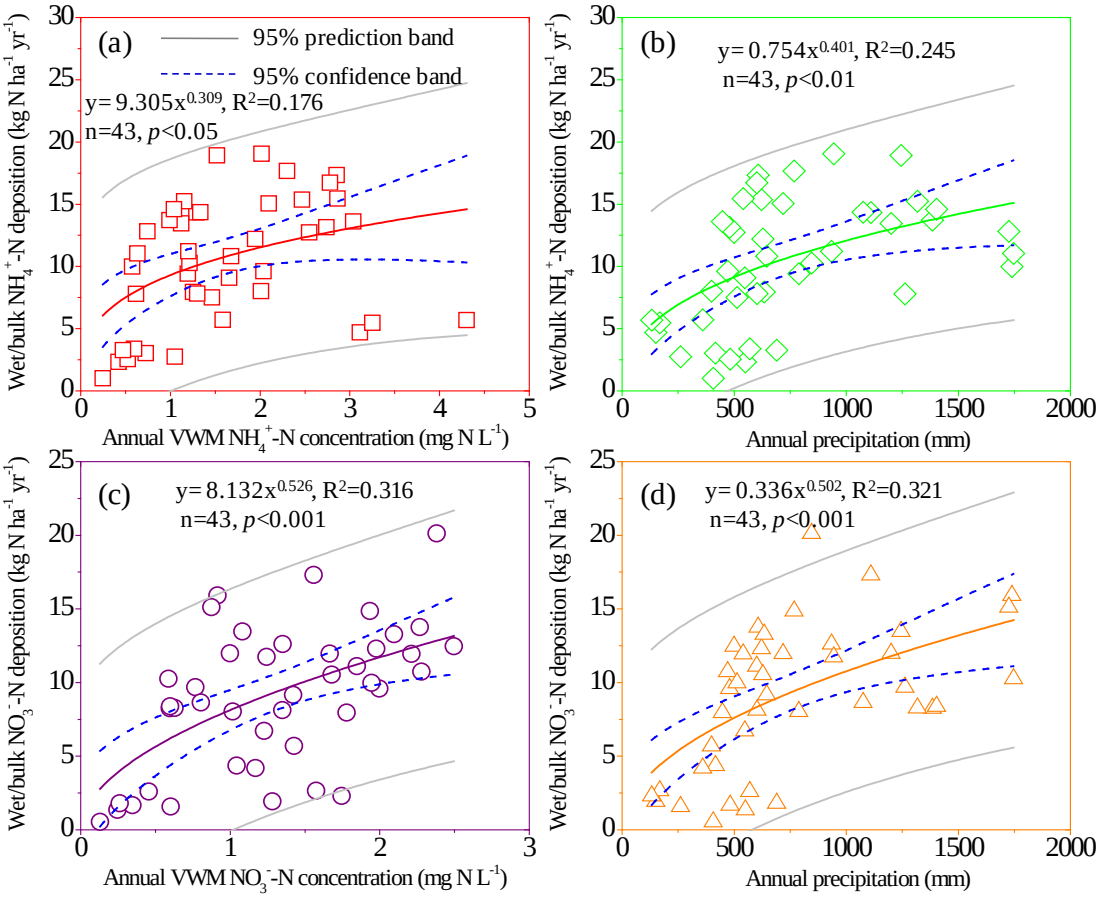
(a)
95% prediction band
95% confidence band
y= 9.305x^0.309, R²=0.176
n=43, p<0.05
Wet/bulk NH4+-N deposition (kg N ha-1 yr-1)
Annual VWM NH4+-N concentration (mg N L-1)
(b)
y= 0.754x^0.401, R²=0.245
n=43, p<0.01
Annual precipitation (mm)
(c)
y= 8.132x^0.526, R²=0.316
n=43, p<0.001
Wet/bulk NO3--N deposition (kg N ha-1 yr-1)
Annual VWM NO3--N concentration (mg N L-1)
(d)
y= 0.336x^0.502, R²=0.321
n=43, p<0.001
Annual precipitation (mm)

Figure 9

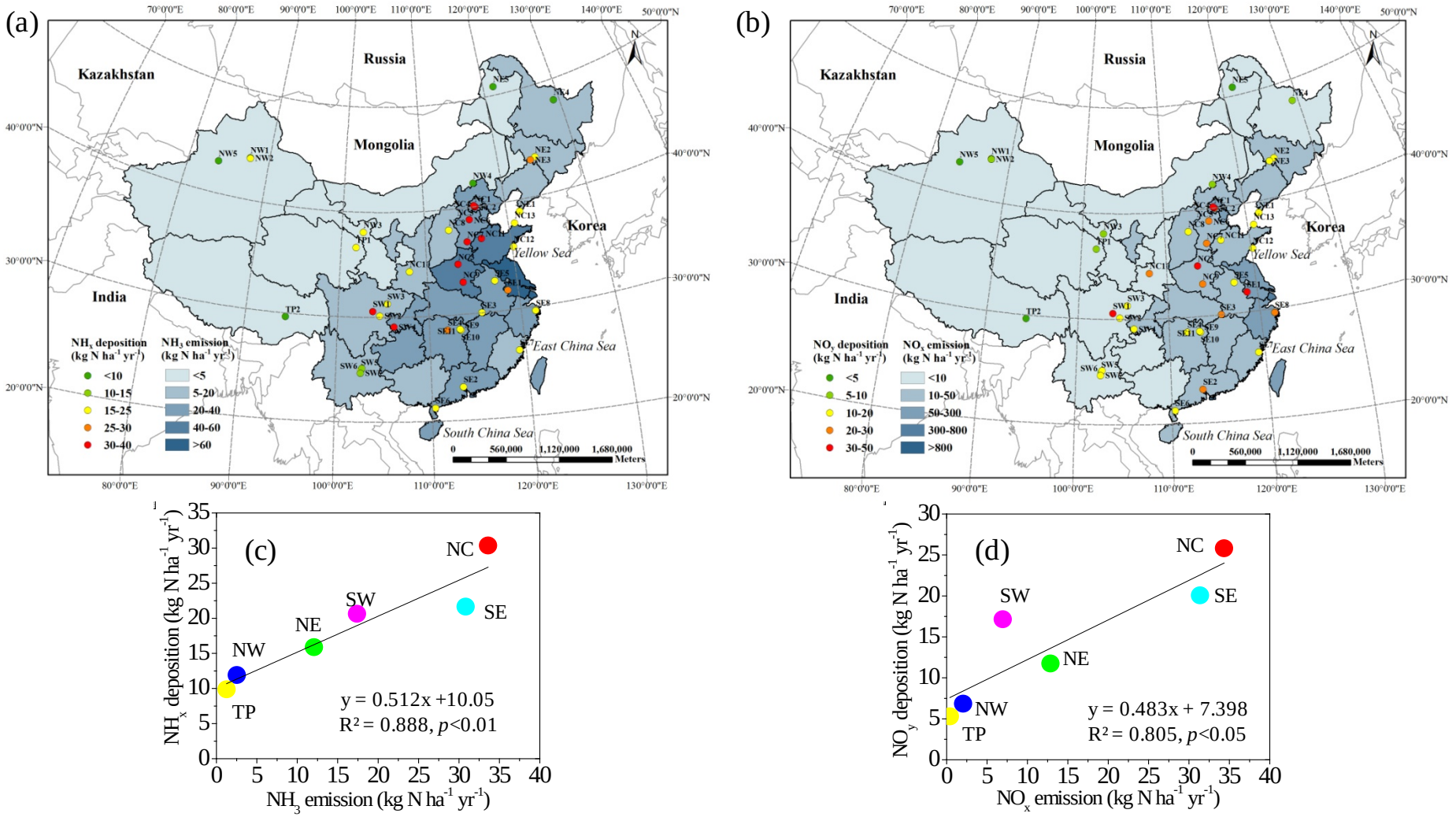
(a)
(b)
(c)
(d)
Kazakhstan
Russia
Mongolia
India
Korea
Yellow Sea
East China Sea
South China Sea
NH3 deposition (kg N ha-1 yr-1)
NH3 emission (kg N ha-1 yr-1)
NOy deposition (kg N ha-1 yr-1)
NOx emission (kg N ha-1 yr-1)
Meters
NH3 deposition (kg N ha-1 yr-1)
NH3 emission (kg N ha-1 yr-1)
y = 0.512x +10.05
R² = 0.888, p<0.01
NOy deposition (kg N ha-1 yr-1)
NOx emission (kg N ha-1 yr-1)
y = 0.483x + 7.398
R² = 0.805, p<0.05
NC
SE
SW
NE
NW
TP

Table 1. Comparison of dry, wet (wet/bulk), and total deposition fluxes of N_r compounds between NNDMN in China and 3 networks in other countries.

Network		Japan EANET network[a]			CASTNET[b]			EMEP[c]			NADMM[d]		
Number of sites or grids		10 sites			130 sites			2447 girds (0.5° × 0.5°)			33 sites		
Observation period		Apr. 2003-Mar. 2008			Apr. 2006-Dec. 2013			Jan. 2003-Dec. 2007			Aug. 2006-Sep. 2014		
N deposition (kg N ha^{-1} yr^{-1})		Dry	Wet	Total	Dry	Wet	Total	Dry	Wet	Total	Dry	Wet/bulk	Total
	Average	3.9	6.6	10.6	3.1	1.3	4.4	3.9	4.8	8.7	18.7	18.2	36.9
	Median	4.1	5.9	11.2	3.0	0.7	4.1	3.7	4.7	8.5	18.7	21.3	36.5
	Max	7.0	15.8	18.2	9.7	10.3	19.6	15.8	16.9	28.0	43.1	32.4	70.9
	Min	1.0	2.1	3.0	0.03	0.1	0.3	0.1	0.6	0.7	1.1	1.5	2.9

[a]The Japan EANET data are sourced from Endo et al. (2011). Gaseous NO_2 was not included in estimates of dry N deposition.

[b] The CASNET data are available online (http://www.epa.gov/castnet/). Gaseous NH_3 was not included in estimates of dry N deposition.

[c]The EMEP data are sourced from Endo et al. (2011), in which the dry and wet deposition amounts at each grid covering 27 EMEP countries were estimated by the unified EMEP models (Simpson et al., 2003).

[d] Only including the rural and background sites in NNDMN.